Altered White Matter Structure In Adults Following Early Monocular Enucleation

Nikita Ann Wong

A THESIS SUBMITTED TO THE FACULTY OF GRADUATE STUDIES IN PARTIAL FULFILMENT OF THE REQUIREMENTS FOR THE DEGREE OF MASTERS

Graduate Program in Psychology
York University
Toronto, Ontario

July 2017

ABSTRACT

Visual deprivation from early monocular enucleation (the surgical removal of one eye) results in a number of long-term behavioural and morphological adaptations in the visual, auditory, and multisensory systems. This thesis aims to investigate how the loss of one eye early in life affects structural connectivity within the brain. A combination of diffusion tensor imaging and tractography was used to examine structural differences in 18 tracts throughout the brain of adult participants who had undergone early monocular enucleation compared to binocularly intact controls. We report significant structural changes to white matter in early monocular enucleation participants that extend beyond the primary visual pathway to include interhemispheric, auditory and multisensory tracts, as well as several long association fibres. Overall these results suggest that early monocular enucleation has long-term effects on white matter structure throughout the brain.

ACKNOWLEDGMENTS

My sincere thanks go first to my supervisor Dr. Jennifer Steeves whose support and guidance throughout my graduate education have been paramount to my development as a researcher. I am grateful for the opportunity to have worked alongside you and to have been a member of your lab. This thesis would not have been possible without you.

I would also like to acknowledge the support of my committee members and all of my participants for the dedication of their time, as well as the Natural Sciences and Engineering Council of Canada and the Canada Foundation for Innovation for funding this research.

I must express my many thanks to my labmates in the Perceptual Neuroscience Lab, Stefania Moro and Sara Rafique. Your constant willingness to provide help and answer my unending stream of questions, along with your advice on all matters has made all the difference over the past two years. I attribute much of my remaining sanity to the laughs we have shared.

Special thanks also go to all of my friends, especially Sarah Wall, who have been endless in their encouragement and who endured countless conversations about graduate school with minimal complaint.

Above all, I have to thank my family – Mom, Dad, and Tianna – for their unwavering love and support over the course of my university career. Without you I would have never made it this far!

TABLE OF CONTENTS

LIST OF FIGURES

ABBREVIATIONS

3D	Three-dimensional
A1	Primary auditory cortex
AD	Axial diffusivity
ATR	Anterior thalamic radiation
BC	Binocular control
BEDPOSTX	Bayesian estimation of diffusion parameters obtained using sampling techniques for modelling crossing fibres
BET	Brain extraction tool
CSF	Cerebral spinal fluid
dLGN	Dorsal lateral geniculate nucleus
DSI	Diffusion spectrum imaging
DTI	Diffusion tensor imaging
FA	Fractional anisotropy
FDR	False-discovery rate
FDT	FSL's diffusion toolbox
FLIRT	FSL's linear registration tool
fMRI	Functional magnetic resonance imaging
FNIRT	FSL's non-linear registration tool
FSL	FMRIB3's software library
HARDI	High angular resolution diffusion imaging

IFOF	Inferior fronto-occipital fasciculus
ILF	Inferior longitudinal fasciculus
JHU	John Hopkins University
LGN	Lateral geniculate nucleus
MD	Mean diffusivity
ME	Monocular enucleation
MGB	Medial geniculate body
MNI	Montreal Neurological Institute
MPRAGE	Magnetisation-prepared rapid gradient-echo
MRI	Magnetic resonance imaging
MRS	Magnetic resonance spectroscopy
OKN	Optokinetic nystagmus
PROBTRACKX	Probabilistic tracking with crossing fibres
RD	Radial diffusivity
SLF	Superior longitudinal fasciculus
SLFt	Superior longitudinal fasciculus (temporal)
TBSS	Tract-based spatial statistics
TTC	Time-to-collision
V1	Primary visual cortex
V2	Secondary visual cortex

CHAPTER I: GENERAL INTRODUCTION

At birth, the visual system is far from mature, and normal development continues well into adolescence. During this period, typical postnatal maturation of the visual system is vulnerable to changes in sensory input, particularly in the first few years of life (e.g., Garey & de Courten, 1983; Huttenlocher & de Courten, 1987). In instances where there is a complete loss of input from a sensory modality (e.g., blindness) neural reorganisation often follows so that other sensory systems recruit brain regions previously engaged by the lost sense (e.g., Merabet & Pascual-Leone, 2010). If vision loss was not complete, but instead reduced only by half, as in the case of the surgical removal of one eye, similar morphological changes might be expected, in order to take full advantage of the remaining sensory inputs. This thesis will consider the morphological adaptations that occur following partial visual deprivation from the loss of one eye early in life.

Monocular enucleation and behavioural adaptations

A unique form of partial visual deprivation is monocular enucleation. Monocular enucleation is the surgical removal of one eye, resulting in the complete deafferentation of 50% of the visual input to the brain. Often the result of retinoblastoma, a childhood cancer of the retina, the removal of an eye is distinct from other forms of monocular visual deprivation, such as cataract (cloudy lens), strabismus (misalignment of the eyes), ptosis (eyelid droop), or anisometropia (unequal focusing power of each eye). Unlike these other types of partial vision loss, in which degraded visual input continues to reach the brain, monocular enucleation completely removes all forms of visual input from one eye, making it a unique model for examining the consequences of the loss of binocularity (Steeves, González & Steinbach, 2008).

Visual adaptations. The long-term behavioural consequences of losing one eye early in life, during postnatal development of the visual system, are well documented. Visually speaking, individuals who have undergone early monocular enucleation exhibit maintained, and in some cases enhanced, performance on most visual spatial tasks, but mild impairments for visual motion perception and oculomotor abilities (reviewed in Kelly, Moro & Steeves, 2012b; Steeves et al., 2008). An early study in participants with only one functional eye reported increased Vernier acuity (i.e., the ability to detect if two edges are misaligned, a hyperacuity) despite normal Snellen acuity compared to monocular viewing controls (Freeman & Bradley, 1980). As Vernier acuity is known to improve with practise (Poggio, Fahle & Edelman, 1992), the enhanced performance of the functionally monocular participants may be attributed to their previous experience viewing with one eye in this manner, in contrast to the monocular viewing controls who rarely perform such tasks with only one eye. A later study in monocular enucleation participants specifically, reported enhanced foveal acuity using Snellen-like letter charts at varying contrasts (between 4% and 96%). At all contrasts except 4%, where binocular performance is superior, individuals who have undergone early monocular enucleation consistently perform better than monocular viewing controls (Reed, Steeves & Steinbach, 1997; Reed, Steeves, Steinbach, Kraft & Gallie, 1996). Similar findings have been reported using illiterate 'E' optotypes at 96%, 13.5%, and 4.7% contrasts with monocular enucleation participants demonstrating improved foveal acuity relative to the monocular acuity of controls. At lower contrasts and 7 degrees of eccentricity, the peripheral acuity of participants who have undergone early monocular enucleation is also improved compared to the monocular control group (González, Steeves, Kraft, Gallie & Steinbach, 2002). In a further study investigating the effects of early monocular enucleation on orientation sensitivity, monocular enucleation

participants showed heightened sensitivity compared to monocular viewing controls on a line orientation task (required participants to align a dot to horizontally and obliquely oriented bars) (Reed, Steinbach, Ono, Kraft & Gallie, 1995).

Contrast sensitivity is another important measure of spatial vision that is enhanced following early monocular enucleation. At 2, 4, and 8 cycles/degree, better contrast sensitivities are observed for monocular enucleation participants compared to the dominant eye of control participants (i.e., monocular viewing control group). Additionally, relative to binocular viewing controls, as well as participants enucleated later in life, participants who had undergone monocular enucleation before the age of two years demonstrated significantly enhanced contrast sensitivity at 4 cycles/degree. Thus contrast sensitivities appear to improve at different rates over the course of development, such that earlier eye loss results in greater improvements in contrast sensitivity over a larger range of spatial frequencies (Nicholas, Heywood & Cowey, 1996).

More complex, higher-level visual functions also remain intact, and are at times enhanced, following early monocular enucleation. For example, participants who have undergone early monocular enucleation exhibit maintained detection and recognition of texture-defined letters relative to controls (Steeves, González, Gallie & Steinbach, 2002). Monocular enucleation participants also demonstrate superior ability to discriminate low-contrast global shape compared to monocular viewing controls, as well as comparable global shape discrimination to binocular viewing controls at all contrasts (Steeves, Wilkinson, González, Wilson & Steinbach, 2004). However, face processing, a unique high-level visual function, appears to be an exception. On tasks requiring participants to process the shape and spacing of internal facial features, participants who have undergone early monocular enucleation show mild impairments relative to both monocular and binocular viewing controls. Specifically, monocular

enucleation participants have significantly slower response latencies, potentially as a means of maintaining their performance accuracy which is comparable to that of controls. However mild, these impairments appear to affect the overall ability for monocular enucleation participants to process faces as a whole (i.e., holistically), rather than in parts. When participants are tested using face analogues (e.g., houses) from a separate visual image category, and which are supported by discrete brain regions (e.g., parahippocampal gyrus, transverse occipital sulcus), these deficits are not replicated, implying that they are face-specific and do not generalise to other categories of visual stimuli (Kelly, Gallie & Steeves, 2012a).

The loss of an eye early in life also has adverse effects on motion perception and oculomotor behaviour (for review, see Kelly et al., 2012b; Steeves et al., 2008). Unlike their enhanced perception of texture-defined letters, monocular enucleation participants demonstrate deficits in motion-defined letter recognition compared to binocular viewing controls. This impairment in motion-defined letter recognition shows a developmental relationship where detection thresholds for form-from-motion are negatively correlated with age at enucleation (Steeves et al., 2002). Additionally, when the perception of time-to-collision (TTC) is measured, monocular enucleation participants show a bias opposite to that of controls, greatly overestimating, instead of underestimating, the TTC of an approaching object (Steeves, Gray, Steinbach & Regan, 2000). An opposite bias for the relative motion of shearing texture stimuli is also observed following early monocular enucleation. Although maintaining relative motion sensitivity comparable to that of controls on this task, monocular enucleation participants tend to judge the bottom half of the texture-defined stimulus as moving faster than the top half (Bowns, Kirshner & Steinbach, 1994). This bias reversal may indicate their attempt to calculate depth perception using motion parallax (a monocular depth cue) in the absence of binocular disparity (a

binocular depth cue). However, more recent findings using a similar task suggest that individuals who have undergone early monocular enucleation have significantly higher relative motion thresholds, and the previously observed perceptual bias for this task was unable to be replicated (González, Lillakas, Greenwald, Gallie & Steinbach, 2014). Participants who have undergone early monocular enucleation have also been found to have elevated global speed discrimination thresholds (Kelly, Zohar, Gallie & Steeves, 2013).

In contrast, separate studies agree that direction discrimination thresholds for coherent horizontal motion are maintained in monocular enucleation participants compared to binocular and monocular viewing controls (Steeves et al., 2002; González et al., 2014). Participants who have undergone early monocular enucleation were again found to exhibit a perceptual asymmetry with elevated motion coherence thresholds for temporalward motion, compared to nasalward motion (Steeves et al., 2002). This asymmetry favouring nasalward motion is similar to an asymmetry observed for eye movement responses measured by optokinetic nystagmus (OKN; Reed et al., 1991). However, this asymmetry was not replicated in later work, and instead a positive correlation between age at enucleation and left-right asymmetry for the motion coherence task was reported (González et al., 2014). An additional assessment also revealed that early monocular enucleation has no effect on smooth pursuit gain relative control participants, indicating that while visual motion perception may be impaired the steady-state smooth pursuit system remains unchanged (González et al., 2014). Lastly, analysis of the horizontal saccade dynamics of participants who have undergone early monocular enucleation revealed no significant changes relative to controls with the exception of saccade latency, which was significantly longer for both monocular viewing groups (i.e., for both monocular enucleation participants and monocular viewing controls) compared to binocular viewing controls (González,

Lillakas, Lam, Gallie & Steinbach, 2013).

Audiovisual adaptations. There is considerable research showing that early blindness results in changes to the other remaining intact sensory systems in order to accommodate for the loss of vision (e.g., Lessard, Pare, Lepore & Lassonde, 1998). Given the importance of integrated audiovisual information in daily life (e.g., on a busy street, our visual system will watch for objects in our path while our auditory system monitors the sounds of nearby traffic), recent research has investigated whether the loss of one eye early in life results in similar adaptations. Recent assessment of binaural sound localisation in participants who have undergone early monocular enucleation revealed significantly greater accuracy, in the central region of space (i.e., within 78 degrees to the left or right of straight ahead), compared to binocular viewing controls, monocular viewing controls, and controls with their eyes shut. Monocular enucleation participants also show enhanced monaural performance, which may be the result of their decreased bias towards localising sounds as 'straight ahead' compared to binocular controls (Hoover, Harris & Steeves, 2012).

The Colavita visual dominance effect, that is the reliable tendency for binocularly intact individuals to preferentially process visual information over auditory information when presented with simultaneous audiovisual input (Colavita 1974; Colavita & Weisberg 1979; Egeth & Sager 1977; Sinnett, Soto-Faraco & Spence, 2008; Spence 2009; Spence, Parise, & Chen, 2011), has also been investigated in participants following early monocular enucleation. Unlike binocular control participants, when asked to detect and discriminate rapidly presented audio, visual, and audiovisual stimuli, monocular enucleation participants do not show the typical pattern of visual dominance. Instead they show equal processing of auditory and visual information, suggesting an increased weighting for the auditory component, or reduced

weighting for the visual component, of audiovisual stimuli (Moro & Steeves, 2012). Additionally, when participants responded to back-to-back presentations of the same auditory, visual, or audiovisual stimuli (i.e., a 1-back task), in order to increase the temporal load for the same task, monocular enucleation participants continued to show equivalent processing of auditory and visual information (Moro & Steeves, 2013).

Visual dominance can also influence performance on audiovisual spatial tasks, for example in the case of the ventriloquism effect. The ventriloquism effect occurs when paired auditory and visual stimuli, which appear to originate from the same location in space, are perceived as a single fused event; but when the two sensory inputs are spatially offset, the fused percept is commonly displaced towards the visual component (Alais, Newell & Mamassian, 2010; Bertelson & Aschersleben, 1998; Welch & Warren, 1980). This effect can be reversed by altering the reliability of the visual component to match that of the auditory cue (Alais & Burr, 2004). When presented with perceptually equated stimuli, individuals who have undergone early monocular enucleation show audiovisual localisation comparable to that of binocular and monocular viewing controls. However, they take significantly longer to localise unimodal visual stimuli compared to unimodal auditory stimuli, and have slower visual response latencies compared to both control groups. Yet despite their slower visual processing speeds, monocular enucleation participants perform audiovisual localisation optimally in accordance with the Maximum Likelihood Estimation model, and thus show normal multisensory integration for this task (Moro, Harris & Steeves, 2014).

Overall, early monocular enucleation results in a number of behavioural changes, both visually and across other sensory systems. Basic and higher-level visual spatial abilities, with the exception of face perception, remain intact following the loss of an eye early in life. Motion

perception and oculomotor abilities, however, appear to be adversely affected by early monocular enucleation, although performance impairments are mild. There is also evidence that individuals who have undergone early monocular enucleation have adaptively altered their ability to process auditory and visual sensory information during multisensory tasks (Kelly et al., 2012b; Steeves et al., 2008). It is likely that these behavioural changes are the result of neural recruitment and reorganisation of cortical and subcortical regions, which allow the brain to adapt after it has been compromised (Guzzetta et al., 2010; Kelly et al., 2012b).

Structural changes following early monocular enucleation

Few studies have investigated the morphological development of the human visual system following partial visual deprivation from early monocular enucleation. The primate visual pathway begins in the retina of each eye with the axons of retinal ganglion cells. These axons converge at the optic chiasm where approximately half of them project ipsilaterally (uncrossed fibres) from the temporal retinae and half project contralaterally (crossed fibres) from the nasal retinae to the lateral geniculate nucleus (LGN). Before reaching the LGN, a subset of these retinogeniculate projections branches off and extends to the superficial layers of the superior colliculus, a laminar midbrain structure located below the LGN. The LGN is the visual nucleus of the thalamus, a subcortical brain structure that is the main relay to and from primary visual cortex (V1). At the LGN visual information is separated into eye-specific layers before projecting via the optic radiations to V1 where the input from each eye first converge at the single cell level. Much of the existing literature has focussed on the structural changes to the anterior portion of the visual pathway (i.e., from the optic tract to the LGN) in late-enucleated individuals. These studies have shown post-mortem that long-term survival from late monocular enucleation results in reduced optic chiasm width (Horton, 1997), degenerated optic tracts, and

transneuronal degeneration of deafferented geniculate cells (Beatty, Sadun, Smith, Vonsattel & Richardson, 1982; Goldby, 1957; Hickey & Guillery, 1979). Transneuronal degeneration of the LGN layers associated with the removed eye has been demonstrated in one early-enucleated adult participant (right-eye removed), however this examination was conducted on the left LGN only (Hickey & Guillery, 1979).

More recently, significant degeneration of the anterior visual system following long-term survival from early monocular enucleation has been demonstrated *in vivo* using magnetic resonance imaging (MRI). The optic nerve, optic chiasm, and optic tract of monocular enucleation participants were all observed to have significantly reduced volumes compared to binocularly intact controls. Analysis of the LGN also revealed bilateral reductions in volume; however, the overall degeneration was considerably less than might have been expected given the 50% loss of visual input. Notably, the volume of the ipsilesional LGN and diameter of the ipsilesional optic tract were significantly less reduced compared to the respective contralesional structures, suggesting the presence of neuroplasticity early in the visual system (Kelly, McKetton, Schneider, Gallie & Steeves, 2014). A later study investigating the consequences of early eye enucleation on cortical regions reported increased surface area and gyrification in visual, auditory (supramarginal), and multisensory (superior temporal, inferior parietal, superior parietal) cortices of monocular enucleation participants. Interestingly, these changes to visual cortex were restricted to primary visual cortex (V1) and inferior temporal cortex of the ipsilesional hemisphere only. The larger surface area and gyrification observed in ipsilesional visual cortex is consistent with the larger optic tract diameter and LGN volume in the same hemisphere (Kelly, DeSimone, Gallie & Steeves, 2015). Thus it appears that the early loss of one eye results in morphological changes throughout the entire visual system.

Given the known behavioural changes in the auditory processing of monocular enucleation participants, structural changes have also been examined in the auditory pathway of this group, specifically at the level of the medial geniculate body (MGB), the subcortical brain structure that relays information to and from primary auditory cortex (A1). Independent of eye of enucleation, the left MGB volume of monocular enucleation participants was significantly larger than the volume of their right MGB, a hemispheric asymmetry that was not present in controls. Additionally, MGB volume was positively correlated with LGN volume, suggesting that following early monocular enucleation, neuroplasticity is increased in both the auditory and visual systems (Moro, Kelly, McKetton, Gallie & Steeves, 2015).

It is clear then that the loss of an eye during postnatal development results in considerable changes in the morphology of both the visual and auditory systems. These anatomical differences are thought to be the basis for the enhanced visual, auditory, and multisensory abilities that have been measured in this group. Such structural changes could be supported by a number of different neural mechanisms. For example, the reduced optic chiasm volume is likely a consequence of the Wallerian degeneration of axons, occurring as a result of the severed optic nerve. However, that the optic nerve of the enucleated eye is still somewhat intact suggests the presence of Wilbrand's knee, where the optic nerve fibres from the remaining eye loop into the enucleated optic nerve before reaching the optic chiasm (Horton, 1997). Furthermore, the reported volume asymmetries for the optic tract, LGN, and MGB could be supported through mechanisms such as neural recruitment of deafferented cells (Grigonis, Pearson & Murphy, 1986; Rakic, 1981) or corticothalamic feedback from primary sensory regions (Barb et al., 2011; Bartlett, 2013; Horton & Hocking, 1998; Kelly et al., 2014; Sloper, 1993; Toosy et al., 2001; Zhang, Suga & Yan, 1997). Impaired synaptic pruning may account for the localised increases in

surface area and gyrification in monocular enucleation participants, likely as a result of the lack of binocular competition from the enucleated eye (Godement, Salaün & Métin, 1987; Grigonis et al., 1986).

Particularly interesting, however, is the idea that changes in white matter can indirectly influence gyrification, which in turn is intimately connected to surface area. As white matter matures, different connections undergo development (e.g., myelination, improved organisation from pruning) causing the cortex to be stretched or pulled, changing its folding patterns (or gyrification), which subsequently influence the surface areas of associated cortical regions (Hilgetag & Barbas, 2006; Van Essen, 1997). Changes in white matter also have the potential to affect feedback mechanisms that may account for other structural changes reported in this group. Therefore, alterations to white matter structure are likely to be linked to many of the known anatomical differences observed following early monocular enucleation. Importantly, white matter maturation continues into adolescence and therefore it is highly possible that its development has been affected by early monocular enucleation (Barnea-Goraly et al., 2005; Gao et al., 2009). Yet, structural connectivity within the brain has not previously been assessed following long-term survival from the removal of an eye. Given the known morphological changes to cortical and subcortical structures in monocular enucleation participants, this thesis examines the question: does early monocular enucleation also affect the structure of white matter within the brain?

Early sensory deprivation and white matter structure

Prior to recent technological developments, investigations into the structure of white matter in the brain were largely limited to post-mortem studies. For several decades monocular enucleation has been a useful method in animal research for investigating the effects of

neuroplasticity on the development of the visual system, including its white matter. In several rodent species (i.e., rats, mice, hamsters), early monocular enucleation has been shown to result in altered retinogeniculate projections, including atrophy and Wilbrand's knee. Significant increases in the number of uncrossed projections contralesionally have also been shown, with these axons innervating regions of the dorsal lateral geniculate nucleus (dLGN) normally reserved for crossed projections (i.e., from the removed eye) (Godement, Saillour & Imbert, 1980; Hsiao, 1984; Lund, Cunningham & Lund, 1973; Toldi, Fehér & Wolff, 1996).

Changes to the geniculocortical projections appear to be more variable across species. Monocularly enucleated rats, for example, exhibit increased scatter (or disorganisation) in the contralesional projections (Jeffery, 1984; Toldi et al., 1996), whereas hamsters that have undergone perinatal monocular enucleation have divergent tracts projecting from the contralesional dLGN, but normal ipsilesional tracts (Trevelyan & Thompson, 1992). On the other hand, in cats, early monocular enucleation does not appear to affect development of the geniculocortical projections (Shook & Chalupa, 1986). Therefore, the changes that occur to white matter structures further down the visual stream are not as consistently affected by the early loss of one eye, potentially as a result of different mechanisms of neuroplasticity, developmental trajectories, or visual pathway anatomy (e.g., differences in the ratio of uncrossed and crossed retinogeniculate projections), across species.

Normal binocular visual input early in life also appears to be crucial for the development of interhemispheric connections. Perinatal monocular enucleation in rats increases the number of interhemispheric connections between the left and right visual cortices, likely as a way for the remaining eye to recruit the largely deafferented visual cortex of the opposite hemisphere (Nys, Scheyltjens & Arckens, 2015; Toldi et al., 1996).

Diffusion tensor imaging

Diffusion tensor imaging (DTI) is a relatively new MRI-based technique developed in the early 1990s (Filler, Tsuruda, Richards, Howe, 1992) for non-invasively mapping structural connections in the living brain using the location, orientation, and preferential axis of diffusion of white matter. To characterise these macro- and microscopic properties, DTI measures the natural movement of water molecules (i.e., diffusion), relying on the fact that water will diffuse differently throughout the brain depending on the type of tissue or the presence of barriers, among other factors. DTI uses a number of images, each sensitised to diffusion in a different direction, to determine the direction and orientation of the diffusion process in a given voxel. This information is summarised in a diffusion tensor model, which uses the lengths and orientations of the three principal axes of an ellipsoid to define the diffusion process (Mori, 2007).

From this information, it is possible to obtain a number of diffusion parameters that describe various aspects of the diffusion process, and which can be useful for making implications regarding the structure of white matter. Fractional anisotropy (FA) is the most widely used diffusion measure, describing the degree of directionality, or anisotropy, of a diffusion process, as a scalar value ranging from zero to one. The FA value will approach zero in brain regions with few barriers (e.g., the ventricles) where water molecules diffuse equally in all directions (i.e., isotropic regions). This is in contrast to areas dense with white matter (i.e., anisotropic regions) where FA will approach one (Mori, 2007). FA is sensitive to differences in microstructure, making it a useful measure when researching changes in white matter structure. However, FA alone cannot specify the nature of the microstructural change and the diffusion parameters from which FA is derived are commonly also measured to help specify the diffusion

process (Jones, Knösche & Turner, 2013).

The average rate of diffusion per voxel, or the average of the three principle eigenvalues from the diffusion tensor, is measured as the mean diffusivity (MD; Mori, 2007). MD reflects changes in water content and cell proliferation in tissue, among other factors, increasing in value in regions where water molecules can diffuse more quickly (e.g., cerebral spinal fluid [CSF]) (Sener, 2001). More specifically, the principal eigenvalue of the diffusion tensor is often referred to as the axial diffusivity (AD), representing the degree of diffusion parallel to the axon (Mori, 2007). Through animal studies, AD has been shown to change with axonal loss or injury, particularly when axon diameter is affected, and with white matter maturation (Budde, Xie, Cross & Song, 2009; Jones et al., 2013; Song et al., 2003). Lastly, radial diffusivity (RD) is the average of the second and third eigenvalues, representing the diffusion occurring perpendicular to the axon (Mori, 2007). Broadly, RD is sensitive to changes in extracellular space, including changes in axon density, axonal calibre, maturation, and in some cases myelination (Jones et al., 2013; Song et al., 2002; Song et al., 2005).

In neurologically intact individuals, several relationships between these diffusion parameters have been reported. For example, in regions with high RD and/or low AD, a reduction in FA often accompanies, whereas increases in MD are commonly seen in areas where RD and/or AD are elevated. These associations can be useful for more precisely identifying the potential mechanisms (e.g., transneuronal degeneration) underlying the change in white matter structure (Jones et al., 2013).

Tractography. Diffusion-weighted data can also be used in tractography, a DTI-based method for creating three-dimensional (3D) reconstructions of fibre tracts and for quantifying the intervoxel connectivity of these projections between brain regions. Currently, the two most

widely used types of tractography are deterministic and probabilistic tractography. Deterministic tractography is conducted using a line propagation technique that relies on the values for AD and FA to define track orientation and termination in a single 'best fit' streamline for each seed point. Although a relatively straightforward method, this raises the potential for false negatives, particularly where fibre bundles closely border grey matter, turn sharply, or enter regions of crossing fibres, causing the FA to drop. Probabilistic tractography on the other hand, models the desired tract using a connectivity index to describe the likelihood of a voxel being part of the tract connecting the specified regions of interest. As numerous probable streamlines are generated, variability is directly incorporated into the calculations, creating a probability map for the tract. This allows probabilistic tractography to better track fibre bundles that enter low FA regions, and makes it less susceptible to noise as it is averaged over the connectivity index. However, probabilistic tractography suffers from distance effects, resulting in the distal portions of fibre bundles having a lower probability of being reached (Jones, 2008; Mori & van Zijl, 2002; Tournier, Mori & Leemans, 2011).

DTI of the visual and auditory systems. Reconstruction of the white matter tracts of the healthy human visual and auditory pathways presents a number of difficulties. In the anterior visual system, the proximity of white matter tracts to the eye muscles, nerves and air-filled cavities complicates the reconstruction of the optic nerves, optic chiasm, and optic tracts (Hofer, Karaus & Frahm, 2010; Staempfli et al., 2007). Likewise considerable interindividual variability and a dense neighbouring network of other white matter bundles present challenges in consistently identifying the precise location and size of the optic radiations (Mandelstam, 2012; Yogarajah et al., 2009). However, with the proper care, recent advancements in DTI methods and processing techniques have made it possible to reconstruct the entire human visual pathway,

and other tracts related to the visual system (e.g., occipito-callosal connections; Dougherty, Ben-Shachar, Bammer, Brewer & Wandell, 2005), with considerable accuracy, as compared to post-mortem findings (Catani & de Schotten, 2008; Catani, Howard, Pajevic & Jones, 2002; de Schotten et al., 2011).

Using DTI and tractography to reliably reconstruct visual white matter pathways not only provides a non-invasive method for assessing qualitative macrostructural changes in white matter, but also provides information regarding its microstructure that is useful for analysing subtle differences in clinical groups or over the course of development, which is not possible with post-mortem examination. For example, significant developmental changes in FA, MD, and RD have been reported in the optic radiations indicating changes in myelination and axon calibre, among other microstructural processes, that are not necessarily reflected in changes to the macrostructure (Dayan et al., 2015).

The main tracts of the human auditory system have also been successfully reconstructed, despite their own complications. For example, compared to their counterpart in the visual system, the auditory radiations are less reliably generated using standard DTI protocols due to the numerous fibre bundles that intersect this relatively small tract (Berman, Lanza, Blaskey, Edgar & Roberts, 2013). Yet recent DTI and tractography reconstructions of the lateral lemnisci and the auditory radiations are comparable with post-mortem data (Catani & de Schotten, 2008; Catani et al., 2002; Javad et al., 2014; Lutz et al., 2007; Roberts et al., 2009). Within the auditory system, DTI has also been used to investigate microstructural developmental changes in its major white matter tracts, revealing that FA increases with maturation of the auditory radiations (Roberts et al., 2009). As well, potential asymmetries in the diffusion parameters have been explored, although no significant hemispheric differences have been identified to date (Lutz et

al., 2007).

DTI and novel tracts. Combined DTI and tractography have also been used in a number of studies to confirm structural connections disputed in conventional MRI and post-mortem findings. For example, the inferior longitudinal fasciculus (ILF; the fibre bundle connecting the occipital and temporal cortices) has been debated in humans, with some results arguing for indirect communication through short fibre bundles instead of a direct cortico-cortical connection. Using DTI several studies have provided support for the existence of a direct occipito-temporal connection, or the ILF (Catani & de Schotten, 2008; Catani et al., 2002; Catani, Jones, Donato & Ffytche, 2003). Similar studies have been instrumental in confirming the inferior fronto-occipital fasciculus (IFOF) in humans (Catani & de Schotten, 2008; Catani et al., 2002; Schmahmann & Pandya, 2007). Recently, new white matter connections have also been postulated, such as a direct cortico-cortical connection between A1 and V1 in humans, as a result of DTI-tractography studies (Beer, Plank & Greenlee, 2011; Beer, Plank, Meyer & Greenlee, 2013).

DTI in clinical populations. DTI and tractography have been of central importance in expanding our understanding of white matter changes in clinical groups, identifying unknown macrostructural differences (e.g., changes in volume, divergent streamlines) as well as providing diffusion parameters from which microstructural properties can be inferred (e.g., changes in myelination). This information has been used to speculate the mechanisms underlying these changes, giving valuable insight into the clinical condition of interest.

A single study has been conducted investigating the short-term consequences of early monocular enucleation (due to retinoblastoma) on white matter development in children. By the age of eight, researchers reported that the optic radiations of children who had undergone early

monocular enucleation were not significantly different than those of healthy control children, based on measurements of FA and MD. Measurements made in the genu and splenium of the corpus callosum were also comparable to controls, although the values in the splenium were considerably more variable for the group of children who had undergone monocular enucleation (Barb et al., 2011).

Much of the remaining DTI literature on visual deprivation has focussed on the consequences of early blindness on white matter development. For example, significantly reduced FA with increased MD and RD has been demonstrated in the optic radiations of early blind and binocularly anopthalmic participants, compared to controls. Together, these changes in the diffusion indices likely reflect axonal degeneration and/or immaturity, presenting two possible accounts for the changes to the white matter. Significant reductions in FA have also been reported in visual cortex (V1 and secondary visual cortex [V2]) of early blind participants, with an accompanying increase in MD in these areas which extends to the posterior corpus callosum. Investigations outside of the visual system have revealed intact connections to temporal and orbital frontal regions from occipital cortex in these individuals. No additional white matter structures have been identified following early blindness (Bridge, Cowey, Ragge & Watkins, 2009; Li et al., 2013; Shimony et al., 2006; Shu, Li, Li, Yu, & Jiang, 2009a; Shu et al., 2009b).

When comparisons are made with other forms of partial visual degradation, such as glaucoma and amblyopia, the white matter abnormalities observed are similar to those following early blindness and suggest similar mechanisms for these changes (Brown, Woodall, Kitching, Baseler & Morland, 2016; Michelson et al., 2013; Murai et al., 2013; Xie et al., 2007; Zhang, Wang, Bai, Ren & Li, 2015). This is in contrast to the findings reported on monocularly

enucleated children, which indicate no significant changes to white matter within the visual system (Barb et al., 2011). This may simply be a consequence of assessing short-term versus long-term neuroplasticity effects; however, previous studies conducted following early monocular enucleation have suggested that the complete loss of an eye results in more compensatory effects of neuroplasticity than those forms of monocular visual deprivation in which degraded visual input continues to reach the brain (e.g., strabismus) (for review see Kelly et al., 2012b; Steeves et al., 2008).

Summary

Monocular enucleation is a unique form of partial visual deprivation resulting in the complete deafferentation of 50% of the visual input to the brain. Previous behavioural studies have demonstrated intact, and in some cases improved, visuospatial and auditory localisation abilities following early monocular enucleation (for review see Kelly et al., 2012b). More recent structural MRI studies have revealed degeneration in the anterior visual system (Kelly et al., 2014), a leftward asymmetry in MGB volume (Moro et al., 2015), and increased surface area and gyrification in primary auditory and visual as well as multisensory cortices (Kelly et al., 2015), in monocular enucleation participants. These morphological changes, presumed to support the reported behavioural differences, could be the outcome of a number of neural mechanisms (e.g., Grigonis et al., 1986; Horton 1997; Rakic, 1981; Sloper, 1993). However, the potential consequences of altered white matter development as a result of early monocular enucleation provides a particularly compelling account for the known structural changes in this group (Barnea-Goraly et al., 2005; Gao et al., 2009; Hilgetag & Barbas, 2006; Van Essen, 1997).

The effects of monocular enucleation on structural connectivity have been investigated extensively in animal models. Consistent atrophy of the anterior visual system has been reported

across rodent species (Godement et al., 1980; Hsiao, 1984; Lund et al., 1973; Toldi et al., 1996) while changes to the geniculocortical tracts and other white matter structures with connections to visual cortex exhibit more variability (Jeffery, 1984; Nys et al., 2015; Shook & Chalupa, 1986; Toldi et al., 1996; Trevelyan & Thompson, 1992). Only one study to date has assessed how the early loss of an eye influences white matter development in humans. Contrary to the animal research, these results revealed no significant changes to the optic radiations or interhemispheric connections. As this study was conducted in children, it is possible that these findings do not fully reflect the long-term effects of neuroplasticity on these visual system structures (Barb et al., 2011). Analyses in adults who experienced early blindness, as well as other forms of monocular visual deprivation, indicate that there are significant differences in the diffusion indices within the visual system and related structures, compared to control participants (e.g., Brown et al., 2016; Shimony et al., 2006). Therefore, it remains unknown how neuroplasticity resulting from early monocular enucleation influences white matter structure over the long-term.

As monocular enucleation results in the complete removal of exactly half of the visual input to the brain, it is a unique model for studying the loss of binocularity. Yet despite the applications of this research for advancing our understanding of other forms of partial visual deprivation, limited research has been conducted in this group. A better understanding of the morphological changes that occur following early monocular enucleation will contribute to our overall understanding of neuroplasticity due to altered sensory input early in life.

Research aims

The aim of this research is to further our understanding of the consequences of neuroplasticity that occur following altered sensory input early in life, specifically following early monocular enucleation. Structural connectivity within the brain has not previously been

assessed long-term following early monocular enucleation. Given the known behavioural and morphological changes (Kelly et al., 2012b; Kelly et al., 2014; Kelly et al., 2015; Moro et al., 2015; Steeves et al., 2008), and the relationship between these structural differences and potential white matter changes (Barnea-Goraly et al., 2005; Gao et al., 2009; Hilgetag & Barbas, 2006; Van Essen, 1997), individuals who have undergone early monocular enucleation might also exhibit significant differences in the structure of their white matter. We will investigate how the loss of one eye early in life and thereby a 50% deafferentation of input to the visual system affects structural connectivity within the brain. Using DTI and tractography we will examine the connectivity of several major white matter tracts of the auditory and visual systems, compared to binocularly intact controls, on measures of FA, MD, AD, and RD. Overall, this thesis will address the question: compared to binocularly intact controls, do participants who have undergone early monocular enucleation exhibit differences in white matter structure that reflect the known morphological changes?

Hypotheses. Specifically, we aim to measure the reciprocal connections between auditory and visual cortical and subcortical regions that have been found to be a) morphologically altered following early monocular enucleation, and b) could support the measured perceptual changes previously observed in this group (for review see Kelly et al., 2012b; Steeves et al., 2008). Seven individual tracts of interest will be investigated as well as a whole brain analysis of 11 additional major white matter structures. Broadly, based on the adaptive behavioural and morphological changes previously reported in this group, we predict that the white matter structure of participants who have undergone early monocular enucleation will be altered relative to controls to take full advantage of the remaining sensory inputs. We expect structural connectivity changes to occur as follows:

Visual system. Analyses of white matter tracts in the visual system will include the optic radiations (LGN-V1), the tracts from V1 to the LGN, and the interhemispheric connections between left and right V1. Recent research in monocular enucleation participants has revealed the anterior visual system to be significantly degenerated, including hemispheric asymmetries in the volumes of the ipsilesional optic tract and LGN, suggestive of neuroplasticity (Kelly et al., 2014). Yet the optic radiations of monocularly enucleated children, as well as their posterior callosal projections, do not indicate any significant differences compared to binocular control children (Barb et al., 2011). These structural connectivity findings are in contrast to previous animal research demonstrating significant changes in both the geniculocortical and callosal projections across rodent species following long-term survival from early monocular enucleation (e.g., Barb et al., 2011; Jeffery, 1984; Trevelyan & Thompson, 1992).

Given the known changes to the anterior visual system of adults who have undergone early monocular enucleation (Kelly et al., 2014), it is possible that the long-term effects of early eye removal on the optic radiations will not reflect those short-term effects reported by Barb et al. (2011). As a result, we predict that the diffusion parameters for the optic radiations of participants who have undergone early monocular enucleation will be significantly different from those of controls, over the long term.

Additionally, given that the increased surface area and gyrification of V1 in monocular enucleation participants (Kelly et al., 2015) may facilitate altered corticothalamic feedback and subsequent changes in connectivity (e.g., Sloper, 1993), we predict that the connection from V1 to LGN will also exhibit significant differences relative to controls.

Lastly, despite the results of Barb et al. (2011) which indicate no significant changes to the splenium in children following early monocular enucleation, the asymmetrical changes to the

surface area and gyrification of V1 after long-term survival (Kelly et al., 2014) could promote significant changes to the interhemispheric V1 connections. Consequently, we also expect to see significant differences in the V1-V1 connection of participants who have undergone early monocular enucleation.

Auditory system. Within the auditory system, the tracts connecting the MGB to A1 (i.e., the auditory radiations) as well as the reverse connection from A1 to the MGB will be investigated. Previous research has demonstrated significant behavioural and structural changes to the auditory system following early monocular enucleation. These changes include enhanced auditory processing (Hoover et al., 2012; Moro & Steeves. 2012; Moro & Steeves, 2013), a leftward asymmetry in MGB volume (Moro et al., 2015), and increased surface area and gyrification in the contralesional supramarginal gyrus (Kelly et al., 2015). Given the direct involvement of the MGB in the tracts of interest, and the role of cortical feedback in developing white matter structure (e.g., Sloper, 1993), we predict that both of the specified auditory tracts of ME participants will have significantly different diffusion parameters compared to those of binocularly intact controls.

Audiovisual system. The tract directly connecting A1 and V1 (Beer et al., 2011; Beer et al., 2013) will be explored in both directions. Monocular enucleation participants demonstrate enhanced auditory processing (Hoover et al., 2012; Moro & Steeves, 2012; Moro & Steeves, 2013) and differences in audiovisual integration (Moro et al., 2014). Research indicates that increased communication between primary sensory regions following sensory deprivation is likely to occur through cortico-cortical, rather than thalamocortical, connections (for review see Bavelier & Neville, 2002). It is possible that the removal of an eye will motivate neural reorganisation in favour of this tract connecting the auditory and visual systems. Therefore, we

predict that participants who have undergone early monocular enucleation will exhibit significant differences in the diffusion parameters for this tract connecting A1 to V1, and similarly V1 to A1, compared to controls.

Other major white matter tracts. A whole brain analysis of 11 major white matter structures will also be conducted, including the following tracts: bilateral anterior thalamic radiations (ATR), bilateral corticospinal tracts, forceps major, forceps minor, bilateral cingulum (cingulate gyrus and hippocampus), bilateral IFOF, bilateral ILF, bilateral superior longitudinal fasciculus (SLF), bilateral temporal SLF (SLFt), and bilateral uncinate fasciculus. Intact connections to the orbital frontal and temporal regions from occipital cortex have been demonstrated in early blind individuals (Shimony et al., 2006), but connections through the splenium of the corpus callosum are varied in children following early monocular enucleation (Barb et al., 2011). As a complete analysis of these 11 tracts has not previously been reported following early visual deprivation, there is the potential for global white matter changes throughout the brain of participants who have undergone early monocular enucleation. However, based on the available research, we predict that any significant differences will be limited to the structures directly connected to occipital cortex.

The results from this research will further our understanding of the morphological changes underlying the behavioural differences previously demonstrated in this group. More broadly, these findings will expand our knowledge of neuroplasticity following altered sensory input early in life, serving as a model for other forms of partial visual deprivation and for the promotion of overall long-term visual health.

CHAPTER II: METHODS

Participants

Early monocular enucleation (ME) participants. Seven individuals (3 female) who had undergone early monocular enucleation at The Hospital for Sick Children participated in this study. All ME participants had been unilaterally eye-enucleated (3 right eye removed) due to retinoblastoma, a childhood cancer of the retina, at a mean age of 24 months (*SD* = 18.1 months, range = 4 – 60 months). Mean age (± SD) at participation was 27.3 ± 10.0 years (range = 16 – 43 years).

Binocular control (BC) participants. Eleven binocularly intact age-matched controls (7 females) were recruited from York University to participate in this study. Control participants ranged in age from 18 to 40 (*M* = 27.8, *SD* = 5.7 years) and had normal Titmus stereoacuity (Stereo Optical Co., Inc., Chicago, IL).

All participants (both ME and BC) had normal or corrected-to-normal acuity as assessed by an ETDRS eye chart (Precision Vision™, La Salle, IL) and had no known contraindications to MRI. All participants gave informed consent prior to their inclusion in this study, which was approved by the York University Office of Research Ethics and conducted in accordance with the 1964 Declaration of Helsinki.

Data acquisition

All scans were acquired on a Siemens MAGNETOM® Tim Trio 3T MRI scanner with a 32-channel head coil (Erlangen, Germany) at the Sherman Health Sciences Research Centre at York University. A high-resolution, T1-weighted 3D magnetisation-prepared rapid gradient-echo (MPRAGE) anatomical image was obtained sagittally, and covering the entire brain, for each participant with the following parameters: rapid gradient echo, 1 mm^3 isotropic voxels, TR =

1900 ms, TE = 2.52 ms, 256 mm FOV, 256 × 256 imaging matrix, and flip angle = 9°. The DTI protocol consisted of a diffusion-weighted echoplanar imaging sequence (TR = 6900 ms, TE = 86 ms, 192 mm FOV, 128 × 128 imaging matrix, voxels 1.5 × 1.5 × 2.0 mm, parallel imaging (GRAPPA with acceleration factor of 3), 64 diffusion directions, *b*-value = 1000 s/mm^2) for 56 contiguous slices, including a single reference volume, b_0 = 0 s/mm^2. Total scan time per participant was approximately 15 minutes.

Data processing

Processing of both anatomical and diffusion-weighted images was conducted using tools from the open source FMRIB3's Software Library (FSL; version 5.0.8, http://www.fmrib.ox.ac.uk/fsl) (Jenkinson, Beckmann, Behrens, Woolrich & Smith, 2012; Smith et al., 2004; Woolrich et al., 2009).

Pre-processing. All scans were first visually assessed for artefacts and as necessary removed from further processing. Pre-processing for the T1-weighted anatomical images consisted of brain extraction to remove the skull and other non-brain tissue using the Brain Extraction Tool (BET; Smith, 2002), and registration of all images to the standard Montreal Neurological Institute (MNI) space template using FSL's Linear Registration Tool (FLIRT; Jenkinson et al., 2002; Jenkinson & Smith, 2001).

Pre-processing of the diffusion-weighted data was performed primarily within FSL's Diffusion Toolbox (FDT). Corrections for potential eddy current distortions, which are stretches and shears induced by the gradient coils, and simple head motion were applied to the diffusion data using affine registration to the b_0 (reference) volume, prior to brain extraction. Registration of these brain-extracted diffusion-weighted images to the MNI space template as well as to the T1-weighted structural image was performed using FSL's Non-Linear Registration Tool

(FNIRT; Andersson et al., 2007a; Andersson et al., 2007b). A diffusion tensor model, that is, a representation of the diffusion process defined using the length and orientation of the three principal axes of an ellipsoid, was then fit at each voxel using a least-squares linear regression approach by running FSL's DTIFIT. Finally, prior to tract reconstruction, Bayesian Estimation of Diffusion Parameters Obtained using Sampling Techniques for modelling Crossing Fibres (BEDPOSTX) was run to estimate the diffusion parameters. BEDPOSTX runs Markov Chain Monte Carlo sampling to build up distributions on diffusion parameters at each voxel and allows modelling of crossing fibres within each voxel of the brain (Behrens, Johansen-Berg, Jbabdi, Rushworth & Woolrich, 2007; Behrens et al., 2003).

Mask creation. In preparation for performing probabilistic tractography, a number of seed (starting point for the tract), termination (stops all tracts upon entry), and exclusion (discards all tracts upon entry) masks were created for the tracts of interest. These included the LGN, V1, MGB, A1, and cerebral white matter (for exclusion purposes) for each hemisphere. Due to the lack of functional and proton density scans for participants, these structures were extracted from the Jülich Histological (Eickhoff et al., 2006; Eickhoff et al., 2007; Eickhoff et al., 2005) and Harvard-Oxford Subcortical Structural (Desikan et al., 2006; Frazier et al., 2005; Goldstein et al., 2007; Makris et al., 2006) atlases available through FSLView. Following extraction, masks were thresholded to a size appropriate for all participants. All masks were overlaid onto each participant's MNI space T1-weighted anatomical image to confirm that they were properly located and sized, prior to tract generation.

Probabilistic tractography. Using FSL's Probabilistic Tracking with Crossing Fibres (PROBTRACKX) tool, probabilistic tractography was performed under default settings, drawing 5000 individual pathways from each voxel in the seed mask at a curvature threshold of 0.2 and a

maximum of 2000 steps. Step length was set at 0.5 mm and distance correction was used. Modified Euler integration for computing probabilistic streamlines (tracts) was selected from advanced options for increased accuracy. Tracking was run from seed to termination masks in each hemisphere separately for all tracts of interest. The appropriate waypoint (requires that all tracts pass through the specified region) and exclusion masks were also set in order to reduce the number of spurious tracts. To investigate the connections from termination to seed masks, the reverse tractography was also performed (Behrens et al., 2007; Behrens et al., 2003).

Extraction of diffusion parameters. Values for the four main diffusion indices were obtained for each tract of interest, in the left and right hemispheres separately, and on an individual basis, using FSL's Tract-Based Spatial Statistics (TBSS). Each participant's MNI space diffusion-weighted data were skeletonized at a threshold of FA > 0.2 to create a mean FA map representing the average FA values in all tracts. The FA, MD, AD, and RD data were then aligned using affine nonlinear registration (FNIRT) and individually projected on to this skeleton (Smith et al., 2006). Masks of the PROBTRACKX generated tracts were used to extract values for the diffusion parameters of the specified tracts of interest.

To examine potential global changes in white matter, the diffusion parameters for 11 additional major white matter tracts (per hemisphere) were extracted by projecting the available standard tracts from the John Hopkins University (JHU) White Matter Tractography atlas (Hua et al., 2008; Mori, Wakana, Van Zijl & Nagae-Poetscher, 2005; Wakana et al., 2007) onto the mean skeleton of each participant.

Statistical analysis

All statistical analyses were conducted using the open source program R (version 3.2.2) (http://www.R-project.org). To assess the potential structural differences in the tracts of interest

following long-term survival from the removal of an eye, ME participants were compared to binocular controls on all diffusion parameters. AD, FA, MD, and RD values were also analysed relative to hemisphere, as well as eye removed for the ME group, for each tract of interest. Independent and repeated-measures *t*-tests, and when necessary their non-parametric counterparts (i.e., the Wilcoxon rank sum [*W*] and Wilcoxon signed rank [*V*] tests), were performed for each of the tracts of interest for this subset of *a priori* comparisons, which included: BC left vs. BC right, ME left vs. ME right, BC left vs. ME left, BC right vs. ME right, and ME ipsilesional vs. ME contralesional. Multiple comparisons were controlled for using the false-discovery rate (FDR) and measures for the appropriate effect sizes were calculated (Cohen's *d* with Hedges *g* correction for small sample sizes, or *r*).

CHAPTER III: RESULTS

Optic radiations (LGN-V1)

A priori pairwise comparisons revealed significantly larger left optic radiation values for MD, $t(10) = 5.874$, $p < .001$, $g = 1.703$ (Figure 1C), and RD, $t(10) = 4.495$, $p = .006$, $g = 1.304$ (Figure 1D), compared to the right optic radiation of binocularly intact participants. Comparable analyses in ME participants revealed a significant hemispheric asymmetry in RD only, $t(6) = 3.909$, $p = .020$, $g = 1.383$, with left-larger-than-right values. Between groups differences were also limited to RD, $t(16) = 2.521$, $p = .038$, $g = 0.937$, such that ME participants had a higher degree of diffusion perpendicular to the axon than controls, however this was significant only in the right hemisphere. No additional significant findings were observed when the ME data were analysed relative to the removed eye (ipsilesional or contralesional).

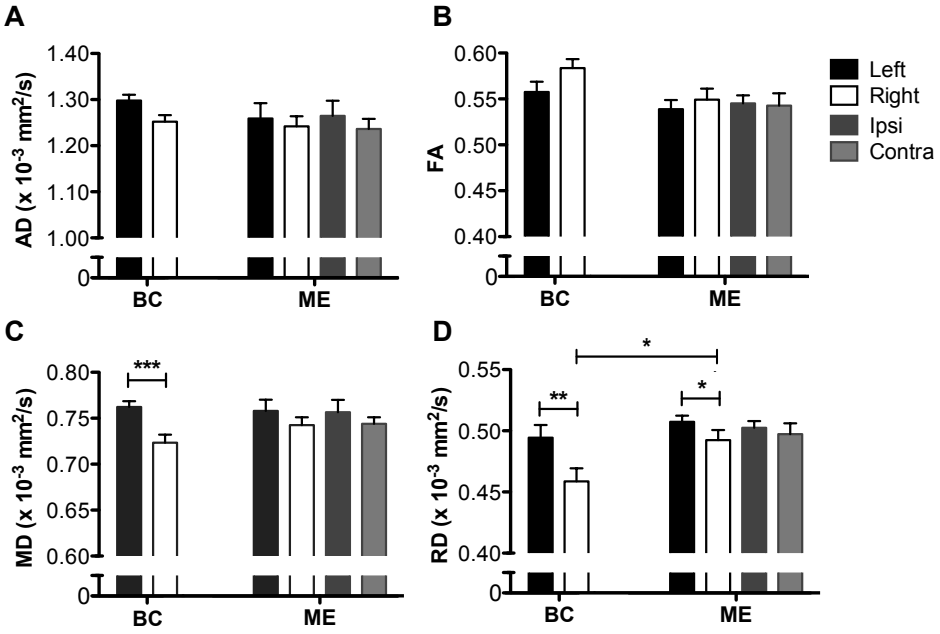

Figure 1. Mean values for the measured diffusion parameters (AD [× 10^{-3} mm^2/s], FA, MD [× 10^{-3} mm^2/s], and RD [10^{-3} mm^2/s]) in the left and right optic radiations for binocularly intact controls (BC) and monocular enucleation participants (ME). Values for the ipsilesional and contralesional optic radiations in ME participants are also reported. Error bars represent standard error of the mean. *BC* = binocular control group; *ME* = monocular enucleation group; *AD* = axial diffusivity; *FA* = fractional anisotropy; *MD* = mean diffusivity; *RD* = radial diffusivity. * $p < .05$; ** $p < .01$; *** $p < .001$.

V1-LGN

Investigation of the connection between V1 and LGN revealed a significant leftward asymmetry in MD for both control, $t(10) = 6.450$, $p < .001$, $g = 1.871$, and ME participants, $V = 28$, $p = .039$, $r = 0.881$ (Figure 2C). Contrary to expectations, values extracted for the ME group did not differ significantly from those of binocularly intact controls, across all diffusion parameters. Analysing the data ipsi- and contralesionally did not reveal any additional significant findings.

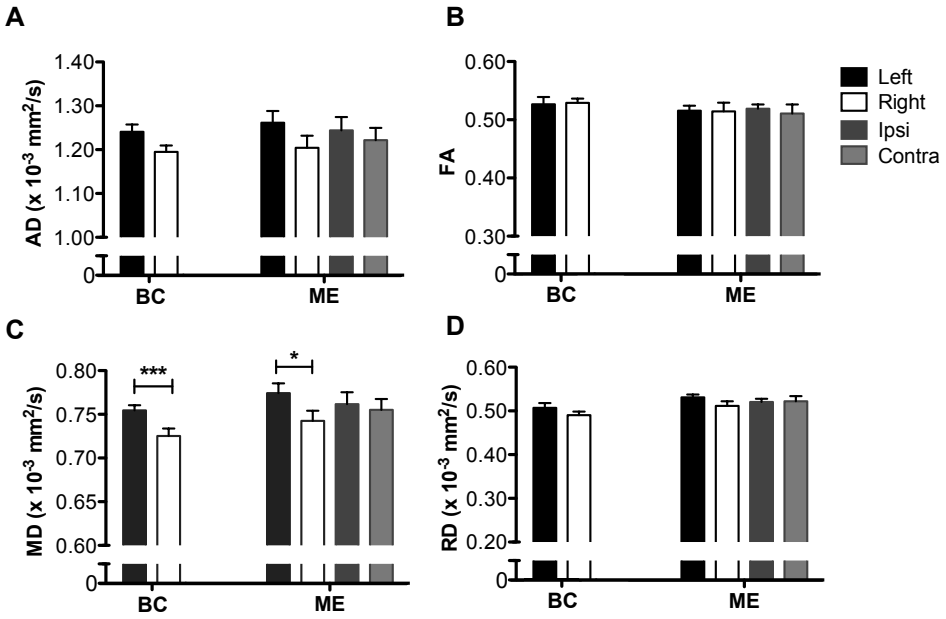

Figure 2. Mean values for the measured diffusion parameters (AD [× 10^{-3} mm^2/s], FA, MD [× 10^{-3} mm^2/s], and RD [× 10^{-3} mm^2/s]) in the left and right tracts connecting primary visual cortex (V1) to the lateral geniculate nucleus (LGN) for binocularly intact controls (BC) and monocular enucleation participants (ME). Values for the ipsilesional and contralesional V1-LGN tracts in ME participants are also reported. Error bars represent standard error of the mean. *BC* = binocular control group; *ME* = monocular enucleation group; *AD* = axial diffusivity; *FA* = fractional anisotropy; *MD* = mean diffusivity; *RD* = radial diffusivity. * $p < .05$, *** $p < .001$.

V1-V1

Significant left-to-right asymmetries were observed for AD, $t(10) = 4.392$, $p = .007$, $g = 1.274$ (Figure 3A), and FA, $t(10) = 4.822$, $p = .004$, $g = 1.399$ (Figure 3B), in the V1-V1 connections of binocularly intact controls. These asymmetries were maintained in ME participants, who likewise showed larger AD, $t(6) = 4.114$, $p = .016$, $g = 1.456$, and FA, $V = 28$, $p = .034$, $r = 0.881$, values when tracking was performed from left V1. These asymmetries were complemented by significantly lower average values for RD, $t(6) = -4.317$, $p = .025$ $g = 1.527$, in the ME group when tracts were reconstructed from the left hemisphere. Between groups pairwise comparisons revealed significantly lower FA values in the ME group compared to controls, when the V1-V1 tracts started in the right hemisphere only, $W = 64$, $p = .034$, $r = 0.995$. Results were not dependent on eye removed.

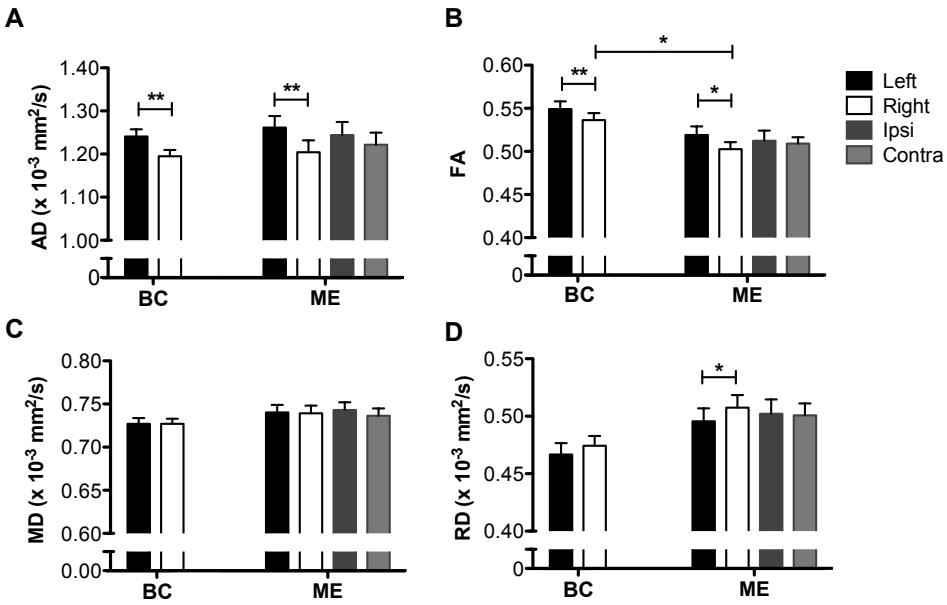

Figure 3. Mean values for the measured diffusion parameters (AD [× 10^{-3} mm^2/s], FA, MD [× 10^{-3} mm^2/s], and RD [× 10^{-3} mm^2/s]) in the interhemispheric tracts connecting left and right primary visual cortex (V1) for binocularly intact controls (BC) and monocular enucleation participants (ME). Values for the tracts connecting ipsilesional and contralesional V1 in ME participants are also reported. Error bars represent standard error of the mean. *BC* = binocular control group; *ME* = monocular enucleation group; *AD* = axial diffusivity; *FA* = fractional anisotropy; *MD* = mean diffusivity; *RD* = radial diffusivity. * $p < .05$; ** $p < .01$.

Auditory radiations (MGB-A1)

Controls exhibited hemispheric asymmetries in the auditory radiations for AD, $t(10) = 3.598$, $p = .024$, $g = 1.044$ (Figure 4A), and MD, $V = 63$, $p = .024$, $r = 0.876$ (Figure 4C), both of which had significantly larger values in the left compared to the right hemisphere tracts. These asymmetries were not present in the auditory radiations of ME participants, yet contrary to hypotheses there were no significant differences in any of the diffusion indices between groups. The hemispheric asymmetries present in controls continued to be absent in the ME group when the data were analysed relative to the removed eye.

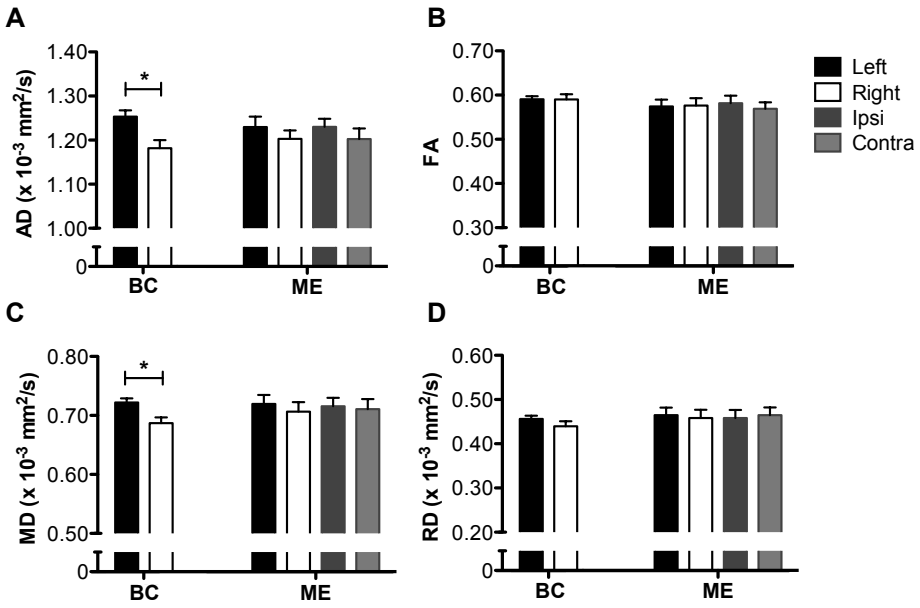

Figure 4. Mean values for the measured diffusion parameters (AD [× 10^{-3} mm^2/s], FA, MD [× 10^{-3} mm^2/s], and RD [× 10^{-3} mm^2/s]) in the left and right auditory radiations for binocularly intact controls (BC) and monocular enucleation participants (ME). Values for the ipsilesional and contralesional auditory radiations in ME participants are also reported. Error bars represent standard error of the mean. *BC* = binocular control group; *ME* = monocular enucleation group; *AD* = axial diffusivity; *FA* = fractional anisotropy; *MD* = mean diffusivity; *RD* = radial diffusivity. * $p < .05$.

A1-MGB

Like the auditory radiations, controls tended to have larger left hemisphere values in the reverse connection between A1 and MGB for both AD, $p = .073$, $g = 0.831$ (Figure 5A), and MD, $p = .085$, $g = 0.830$ (Figure 5C). Again, ME participants did not show these tendencies towards hemispheric asymmetries, and there were no significant between groups findings. Comparisons conducted ipsi- and contralesionally did not reveal any significant results.

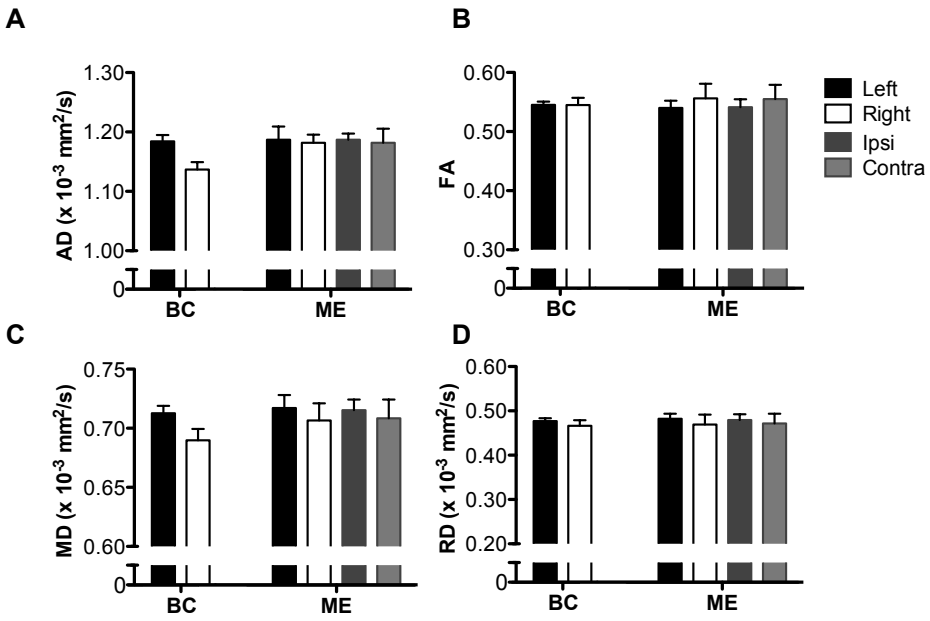

Figure 5. Mean values for the measured diffusion parameters (AD [× 10^{-3} mm^2/s], FA, MD [× 10^{-3} mm^2/s], and RD [× 10^{-3} mm^2/s]) in the left and right tracts connecting primary auditory cortex (A1) to the medial geniculate body (MGB) for binocularly intact controls (BC) and monocular enucleation participants (ME). Values for the ipsilesional and contralesional A1-MGB tracts in ME participants are also reported. Error bars represent standard error of the mean. *BC* = binocular control group; *ME* = monocular enucleation group; *AD* = axial diffusivity; *FA* = fractional anisotropy; *MD* = mean diffusivity; *RD* = radial diffusivity.

A1-V1

Within groups pairwise comparisons for binocularly intact participants revealed significantly larger left hemisphere, compared to right hemisphere, values for MD, $t(10) = 4.910$, $p = .003$, $g = 1.424$ (Figure 6C), and RD, $t(10) = 3.617$, $p = .024$, $g = 1.049$ (Figure 6D), for the tracts connecting A1 to V1. These hemispheric asymmetries were not present in ME participants, and were absent even when the data were analysed relative to the removed eye. Inconsistent with hypotheses, there were no significant differences for any of the diffusion parameters between controls and participants who had undergone early monocular enucleation.

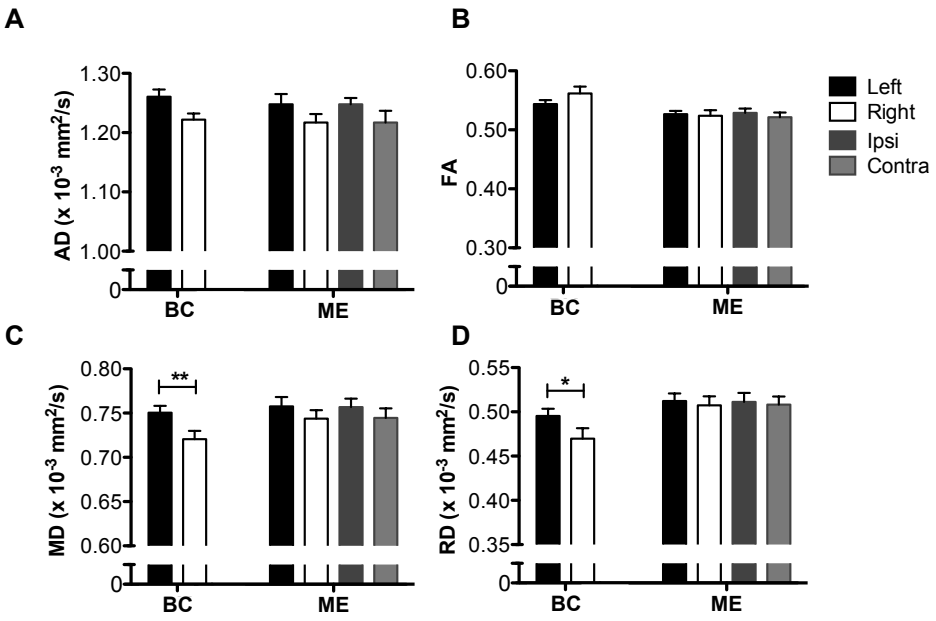

Figure 6. Mean values for the measured diffusion parameters (AD [× 10^{-3} mm^2/s], FA, MD [× 10^{-3} mm^2/s], and RD [× 10^{-3} mm^2/s]) in the left and right tracts connecting primary auditory cortex (A1) to primary visual cortex (V1) for binocularly intact controls (BC) and monocular enucleation participants (ME). Values for the ipsilesional and contralesional A1-V1 tracts in ME participants are also reported. Error bars represent standard error of the mean. *BC* = binocular control group; *ME* = monocular enucleation group; *AD* = axial diffusivity; *FA* = fractional anisotropy; *MD* = mean diffusivity; *RD* = radial diffusivity. * $p < .05$; ** $p < .01$.

V1-A1

Controls exhibited the same leftward asymmetries in MD, $t(10) = 3.369$, $p = .036$, $g = 0.977$ (Figure 7C), and RD, $t(10) = 3.970$, $p = .013$, $g = 1.151$ (Figure 7D), for the reverse connection from V1 to A1 as they did when tracking was performed from A1 to V1. Again, the ME group did not demonstrate these asymmetries, but rather showed significantly larger values in the left V1-A1 compared to right V1-A1 for AD, $t(6) = 3.744$, $p = .048$, $g = 1.325$ (Figure 7A). Significant between groups comparisons were limited to smaller FA values in ME participants compared to control participants in the right V1-A1 tract only, $t(16) = -3.166$, $p = .030$, $g = 1.347$. Results were not dependent upon the eye removed.

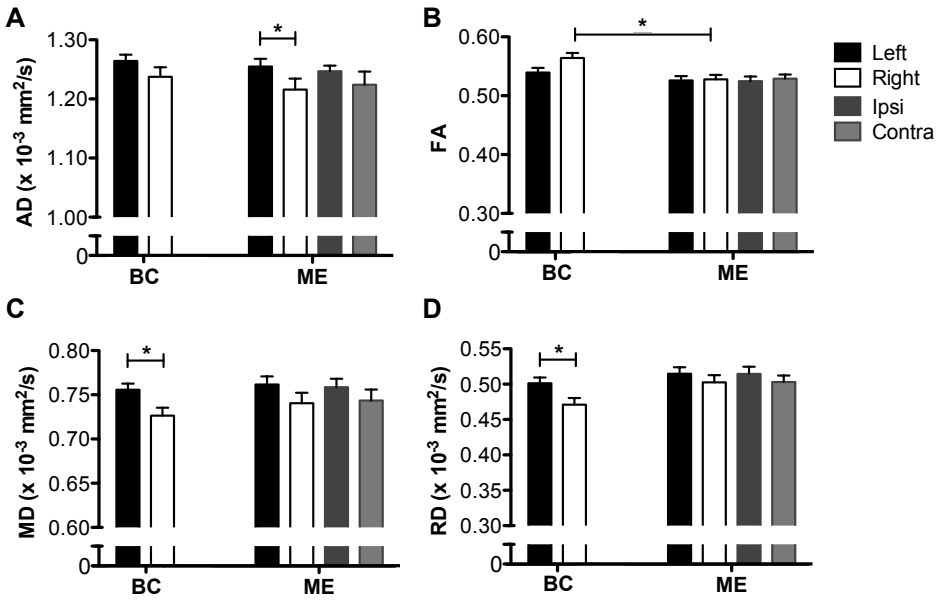

Figure 7. Mean values for the measured diffusion parameters (AD [× 10^{-3} mm^2/s], FA, MD [× 10^{-3} mm^2/s], and RD [× 10^{-3} mm^2/s]) in the left and right tracts connecting primary visual cortex (V1) to primary auditory cortex (A1) for binocularly intact controls (BC) and monocular enucleation participants (ME). Values for the ipsilesional and contralesional V1-A1 tracts in ME participants are also reported. Error bars represent standard error of the mean. *BC* = binocular control group; *ME* = monocular enucleation group; *AD* = axial diffusivity; *FA* = fractional anisotropy; *MD* = mean diffusivity; *RD* = radial diffusivity. * $p < .05$.

Other major white matter tracts

An analysis of 11 additional major white matter structures revealed significant differences throughout the brain of ME participants, outside of the *a priori* tracts of interest. Similar to the findings obtained for the PROBTRACKX reconstructed tracts, for a number of these structures the ME group did not exhibit the significant asymmetries that were present in the control group. In binocularly intact participants only, larger left hemisphere values for AD, MD, and RD were found in the hippocampal portion of the cingulum (AD: $t(10) = 4.937$, $p = .003$, $g = 1.432$; MD: $V = 66$, $p = .005$, $r = 0.876$; RD: $t(10) = 3.168$, $p = .050$, $g = 0.919$), the IFOF (AD: $t(10) = 3.491$, $p = .029$, $g = 1.013$; MD: $V = 66$, $p = .019$, $r = 0.876$; RD: $t(10) = 6.919$, $p < .001$), and the ILF (AD: $t(10) = 3.422$, $p = .033$, $g = 0.993$; MD: $t(10) = 4.921$, $p = .003$, $g = 1.427$; RD: $V = 66$, $p = .019$, $r = 0.876$). Additionally, in the SLF and SLFt, ME participants did not demonstrate the asymmetrical AD values found in controls, $t(10) = 3.319$, $p = .007$, $g = 0.963$, however the significant asymmetries in FA (BC: $t(10) = -4.224$, $p = .002$, $g = 1.225$; ME: $t(6) = -5.083$, $p = .002$, $g = 1.799$), MD (BC: $t(10) = 6.778$, $p < .001$, $g = 1.966$; ME: $t(6) = 3.297$, $p = .016$, $g = 1.167$), and RD (BC: $t(10) = 6.386$, $p < .001$, $g = 1.852$; ME: $t(6) = 5.002$, $p = .002$, $g = 1.770$) were consistent across groups. This lack of asymmetries suggests widespread changes to important white matter tracts outside of the primary visual pathway following early monocular enucleation. Additional changes in these tracts included a significant group difference in the ILF, which indicated significantly smaller FA in ME participants compared to control participants in the right ILF only, $W = 71$, $p = .009$, $r = 0.878$. As well, a significant effect of eye removed was seen in the IFOF, with MD values being larger in the ipsilesional tract compared to the contralesional tract, $W = 16.5$, $p = .019$, $r = 0.878$.

Analysis of the cingulum (cingulate gyrus), the uncinate fasciculus, the ATR, the

corticospinal tract, and the forceps major and minor, revealed the same hemispheric asymmetries (or lack thereof) in both control participants and ME participants, with no significant between groups differences. There was no significant effect of eye removed for any of these tracts.

CHAPTER IV: DISCUSSION

The current thesis investigated the long-term consequences of early monocular enucleation on structural connectivity throughout the brain. Diffusion-weighted images were acquired in participants who had undergone early monocular enucleation and binocularly intact controls, and probabilistic tractography was used to reconstruct the tracts of interest. Potential changes to white matter structure were compared between and within groups on measures of FA, AD, MD, and RD for a total of 18 tracts throughout the brain. It was hypothesised that ME participants would show significant differences in the diffusion indices relative to controls in the seven *a priori* tracts of interest, as well as the major white matter tracts with direct connections to occipital cortex, given that one half of the visual input to the brain was removed during early postnatal maturation.

Three broad patterns of results were apparent across the sets of tracts investigated: tracts that showed differences between groups, tracts that in ME participants lacked the hemispheric asymmetries found in control participants, and tracts which were unchanged across the participant groups. These between groups differences and lack of asymmetries are taken as evidence for structural changes to white matter following early monocular enucleation, although on the whole, there were fewer differences between ME and control participants than originally expected. Overall, the results of this study suggest that early monocular enucleation has distal effects on white matter structure both within the visual system, as well as other sensory systems, and visually dependent major white matter tracts.

Review of diffusion indices

A review of the diffusion indices, the structural changes they can represent, and the potential mechanisms for these changes, will be useful prior to discussion of the present results.

The diffusion-derived measures of interest in this study are FA, MD, AD, and RD. While these indices can provide important information regarding white matter microstructure, caution must be used when interpreting the structural differences that accompany changes in these parameters. For any given change in each of FA, MD, AD, and RD, there are numerous potential structural correlates. Recall that changes in FA represent a general difference in white matter microstructure, and that through the use of AD and RD this difference might be further specified (Mori, 2007). Broadly, AD and RD represent changes to intra- and extra-axonal space, respectively, although they overlap considerably (Le Bihan, 2003; Pierpaoli & Basser, 1996). Both of these parameters can also increase or decrease in cases of axonal pathology, making interpretation difficult. Briefly, AD will increase in cases of axonal injury or inflammation (Song et al., 2002), but also when fibre coherence is improved (Dubois et al., 2008; Takahashi, Ono, Harada, Maeda & Hackney, 2000). Reductions are commonly observed with development when the growth of neurofibrils and glial cells restrict diffusion parallel to the axon (Kinoshita, Ohnishi, Kohshi & Yokota, 1999). Increased RD on the other hand is commonly associated with impaired or damaged myelin, but also correlates positively with fibre calibre (Jones et al., 2013; Schmierer et al., 2007; Song et al., 2002; Song et al., 2005). Axonal loss, or degeneration, results in higher AD and RD, while decreased axonal density elevates RD but causes a reduction in AD. As MD is a linear combination of AD and RD (i.e., $[\lambda_1 + \lambda_2 + \lambda_3]/3$), it is subject to all of the factors that influence both AD and RD. In the absence of additional post-mortem research across different pathological conditions, the precise structural difference a change in diffusion parameters represents for a given group and the associated mechanisms underlying these changes, remain indeterminate (Jones et al., 2013). Nevertheless, with the appropriate caveats, there are a number of relations between changes in diffusion indices, the associated structural

differences, and suggested mechanisms.

There are several consistent patterns of change in the diffusion indices following early blindness, or partial vision loss from glaucoma and amblyopia. The optic radiations of these individuals show reliable reductions in FA compared to control participants, and when they are analysed, higher MD and RD. Together, this pattern of results is often taken to indicate neurodegeneration, particularly in early blind participants who also exhibit anterior visual system atrophy. Based on the reduction (or loss) of visual input to the brain, axonal degeneration and immaturity are the two most commonly presented mechanisms to account for such changes. Post-mortem and neuroimaging studies have demonstrated degeneration of the LGN following lesions to the optic nerve in cases of early blindness and optic neuritis (e.g., Beatty et al., 1982; Ciccarelli et al., 2005; Shimony et al., 2006; Shu et al., 2009a). It has been postulated that through transneuronal degeneration this damage could extend to structures further down the visual pathway, such as the optic radiations, and be reflected in changes to the diffusion parameters (Boucard et al., 2016; Shu et al., 2009a). As degeneration would result in both axonal loss and reduced axon density, and given that RD characterises extra-axonal space, it is common for RD to increase in such cases (Jones et al., 2013).

However, evidence for the immaturity hypothesis also has merit, especially in forms of partial visual deprivation that are less likely to have atrophied anterior visual system structures. Loss of visual input (either partial or complete) early in life has the potential to interfere with the typical development of the optic radiations, as a result of decreased activity and visual experience (Alix & Domingues, 2011; Boucard et al., 2016; Sengpiel & Kind, 2002). Although sensory systems white matter, such as the optic radiations, are known to mature early in life (often before three years of age; Kinney, Kloman & Gilles, 1988), refinement of the fibre

bundles (e.g., through pruning), including myelination, that are necessary for normal maturation, are experience-dependent (e.g., Alix & Domingues, 2011; Sengpiel & Kind, 2002). Therefore, a reduction or absence of visual input, resulting in decreased activity throughout the visual pathway may impede the later stages of development of the optic radiations, and other white matter structures. Axonal immaturity is accompanied by higher RD and lower FA that reflect the increased disorganisation of the fibre bundle caused by the incomplete pruning and myelination processes (Boucard et al., 2016; Jones et al., 2013; Shu et al., 2009a). This is supported by developmental research in white matter of healthy individuals. In structures throughout the brain, white matter shows an increase in FA and decrease in MD with age that is largely driven by a reduction in RD, rather than a change in AD (e.g., Dayan et al., 2015; Schmithorst, Wilke, Dardzinski & Holland, 2002; Schmithorst &Yuan, 2010). While this age-related decrease in RD is often ascribed to increased myelin, the relationship between RD and myelin integrity is correlational and the precise nature of these concomitant changes has yet to be ascertained (Jones et al., 2013; Song et al., 2002).

Notably, reduced visual pathway activity may also cause axonal degeneration as a result of disuse atrophy, both of which can account for alterations to distal tracts related to the visual system (Boucard et al., 2016). Following early blindness, for example, the posterior corpus callosum exhibits significantly lower FA (Shimony et al., 2006). If transneuronal degeneration changed the structure of the optic radiations, Wallerian degeneration may take place in later visual system structures (e.g., V1), spreading to other axons, including those that have interhemispheric projections between left and right V1, and resulting in reduced FA in these tracts. On the other hand, the reduction in visual input is likely to be reflected in reduced V1 activity, which could impede the normal maturation of related tracts outside of the primary visual

pathway, such as the corpus callosum, resulting in changes similar to those observed in the optic radiations (Boucard et al., 2016; Shu et al., 2009a).

Visual system tracts of interest

Optic radiations. Analysis of the optic radiations revealed significantly higher RD in participants who had undergone early monocular enucleation compared to binocularly intact controls in the right hemisphere tract only. Interestingly, ME participants did not show the significant leftward asymmetry in MD that was found in controls; however both groups had a significant left-higher-than-right asymmetry in RD. In controls, this asymmetrical occurrence of RD in the optic radiations likely influenced the higher MD in the left hemisphere, but as to whether these are normal developmental asymmetries remains a matter of debate. Average values for the diffusion parameters in the optic radiations are variable throughout the literature, although the values for the current study do fall within the range of those previously reported. Variations in DTI protocol and methodology, such as fewer diffusion directions or different participant samples, can likely account for these deviations in the diffusion parameters (Dayan et al., 2015; de Schotten et al., 2011; Sherbondy et al., 2008).

Within the ME group, the significantly greater RD in the right optic radiation likely drove the MD higher in the same hemisphere, eliminating the leftward asymmetry observed in controls. As mentioned in the review of the diffusion parameters at the beginning of this chapter, a significant increase in RD can indicate a number of structural changes including axonal loss or increased axonal diameter, among other factors that increase the extra-cellular space around axons (Le Bihan, 2003; Pierpaoli & Basser, 1996). In cases of long-term visual deprivation, higher RD values are commonly interpreted as the result of transneuronal degeneration or axonal immaturity, especially when accompanied by a reduction in FA (e.g., Boucard et al., 2016; Shu

et al., 2009a). Given the atrophy previously demonstrated in the anterior visual system following early monocular enucleation, including the LGN (Kelly et al., 2014), transneuronal degeneration could certainly account for the increased RD in the optic radiations observed here. Of course, the early loss of 50% of visual input to the brain also has the potential to significantly reduce visual pathway activity and interfere with the normal development of this tract. However, RD has also been shown to positively correlate with axonal calibre (Schmierer et al., 2007), and thus this significant increase could similarly indicate a compensatory mechanism.

To an extent, these results support those of Barb and colleagues (2011) who found no significant differences in FA or MD between monocularly enucleated children and control children, in keeping with the current study. However, if there were any significant hemispheric asymmetries, they were not reported, and as neither AD nor RD were measured, it is difficult to make further comparisons (Barb et al., 2011). Relative to early blind individuals and participants with partial vision loss from glaucoma and amblyopia, who demonstrate significant reductions in FA and concomitant increases in MD and RD in the optic radiations (e.g., Shimony et al., 2006; Shu et al., 2009a; Shu et al., 2009b; Xie et al., 2007; Zhang et al., 2015), the changes reported here in ME participants are considerably less severe. Together, the present findings suggest that the effects of early monocular enucleation on the structure of the optic radiations occur over the long term, and are less pervasive than the changes following other forms of vision loss.

Aside from the significant between groups difference in RD the optic radiations following early monocular enucleation remain intact. Notably, there were no significant changes in FA or AD between or within groups, and although the ME group did not demonstrate the leftward asymmetry in MD the values in both the left and right hemispheres did not differ significantly from those of control participants. The fact that the optic radiations were largely

unchanged is particularly significant given the changes observed in the anterior visual system of ME participants (Kelly et al., 2014). Considering the role the optic radiations play in relaying information from the subcortical LGN to V1, the preservation of this key visual system tract could contribute to the intact visuospatial processing previously demonstrated in this group (Kelly et al., 2012b; Steeves et al., 2008).

V1-LGN. Unlike the optic radiations, and contrary to hypotheses, the tract connecting V1 to the LGN appears to be unaffected by early monocular enucleation, showing neither significant between groups differences, nor an absence of hemispheric asymmetries in ME participants, as was observed with MD in the optic radiations. Rather, a leftward asymmetry in the average diffusivity (MD) was found in both groups. A number of mechanisms could account for the larger MD in the left V1-LGN projections, however given its presence in both groups it is possible that this asymmetry is naturally occurring in this tract. To our knowledge, none of the diffusion indices have previously been assessed in this tract, and thus there are no established values or trends with which to compare the current results.

Corticothalamic feedback may be responsible for the preservation of this tract despite the atrophy of the anterior visual system (Kelly et al., 2015; Kelly et al., 2014) and changes to the optic radiations (Beatty et al., 1982). As previous research has demonstrated, visual functioning is largely intact, and in some cases enhanced, following early monocular enucleation (for review see Kelly et al., 2012b; Steeves et al., 2008). The normal maturation, including myelination, of white matter is experience-dependent, with connections being strengthened and pruned through neuronal activity (Alix & Domingues, 2011; Sengpiel & Kind, 2002). If functional activity in early visual cortex was in keeping with that required to support maintained corticothalamic feedback to the LGN, then this might account for the unchanged structure of the V1-LGN tract

of ME participants, irrespective of the other structural changes to the visual system.

Notably, the increased surface area and gyrification of ipsilesional V1 previously demonstrated in ME participants (Kelly et al., 2015) do not appear to have affected the white matter tract connecting V1 and the LGN. Morphological changes to cortex do not necessarily influence function (Bridge et al., 2009; Rakic, 1988) and therefore, it is possible that the known structural changes to V1 did not influence visual functioning to an extent which influenced feedback to the LGN. Future studies should use functional MRI (fMRI) to investigate the activity of V1 in ME participants and the potential for any changes to influence the morphology of this group.

V1-V1. The interhemispheric connection between left and right V1 was significantly asymmetric in both control and ME participants for AD and FA, with larger values apparent when tracking was performed from left, rather than right, V1. In ME participants only, the opposite asymmetry was also observed for RD. A significant between groups difference was revealed, with ME participants having significantly smaller FA values relative to controls, when tracking was conducted right-to-left. The AD and FA asymmetries present in controls as well as ME participants may reflect inherent developmental asymmetries resulting from hemispheric differences in grey matter or function (Hellige, 1993), which are maintained in both groups. To date, the interhemispheric connections between V1 have not been widely investigated using tractography that directly seeds left and right V1 (Dougherty et al., 2005). Much of the DTI literature reconstructing posterior interhemispheric connections has examined the posterior segment of the corpus callosum, or the splenium, which has projections to parietal and temporal cortex as well as V1, making accurate comparisons difficult (Lebel, Caverhill-Godkewitsch & Beaulieu, 2010; Schulte, Sullivan, Müller-Oehring, Adalsteinsson & Pfefferbaum, 2005; Takao

et al., 2011). The splenium in particular is also subject to considerable interindividual variation (Hellige, 1993; Putnam, Steven, Doron, Riggall & Gazzaniga, 2010). These factors could reconcile the marginally lower FA and MD values that were found in control participants as compared to previous averages in similar tracts (e.g., posterior corpus callosum) in healthy individuals (Lebel et al., 2010; Schulte et al., 2005).

It is likely that the significant between groups difference in FA was the consequence of the significant right-to-left asymmetry for RD in ME participants, which caused FA in the same V1-V1 tract to decrease. This reduction in FA suggests that there is some form of microstructural difference between ME participants and control participants in the interhemispheric V1 connections. As there are a number of reasons for RD to increase, there are a number of possible changes that may have occurred to this connection following the early loss of one eye. It may be that this change is an extension of the right hemisphere increase in RD in the optic radiations. Altered posterior commissural projections have been related to changes in the optic radiations in both early blind and glaucoma participants. Transneuronal degeneration of the optic radiations could result in Wallerian degeneration of neighbouring axons in V1 which extend in to the opposite hemisphere. Likewise, a reduction in visual system activity is likely to be reflected in V1 from which the interhemispheric V1 connections project. If altered visual input were the cause of the changes to the optic radiations it could also influence the change to the V1-V1 tracts resulting in immaturity that is reflected in fibre disorganisation (i.e., lowered FA) from impaired pruning or myelination (Boucard et al., 2016; Shimony et al., 2006). On the other hand, RD could represent the development of new interhemispheric projections, as has been previously demonstrated in monocularly enucleated hamsters and rats. Rather than showing an interruption in the development of the interhemispheric connections between visual regions, new patterns of

projections emerge; however, whether this adaptive or maladaptive is unclear (O'Brien & Olavarria, 1994; Olavarria & Malach, 1987). As RD represents the diffusion perpendicular to the main fibre bundle, it is possible that an increase in this measure could indicate the development of projections in a different direction, which would also cause the overall directionality of the diffusion in the fibre bundle to decrease.

As with the optic radiations, the significant changes to the interhemispheric V1 connections of ME participants are not pervasive. This is in contrast to the differences following early blindness and other forms of partial vision loss, which exhibit substantially larger bidirectional reductions in FA and accompanying increases in MD (Shimony et al., 2006). There is, however, some correspondence between these results and those of Barb et al. (2011) who found considerably more variation in FA and MD values in the splenium of children who have undergone early monocular enucleation. The findings presented here may be an extension of these results, with the variable values seen shortly following enucleation failing to reach normal standards over the long-term (Barb et al., 2011). However, as mentioned previously, the V1-V1 tract reconstructed in the current study and other posterior connections may exhibit considerable differences, and comparisons should be made cautiously (Lebel et al., 2010; Putnam et al., 2010; Schulte et al., 2005; Takao et al., 2011).

Overall, it appears that early monocular enucleation has distal effects on visual system white matter, which extend to the interhemispheric V1-V1 connections. Like the optic radiations, these effects take place in the later stages of maturation (i.e., after childhood) and are less severe than changes reported following other forms of vision loss. That the interhemispheric V1 connections of ME participants are largely intact, may contribute to their normal visual spatial processing by maintaining relatively normal communication between the primary visual cortices

(Kelly et al., 2012b; Steeves et al., 2008). Again, as with the V1-LGN tracts, there was no effect of eye removed or the increased surface area and gyrification of ipsilesional V1 on these tracts (Kelly et al., 2015), suggesting that separate mechanisms may influence the development of grey and white matter in the visual system following early loss of one eye.

Nonvisual tracts of interest

Outside of the visual system, tracts were reconstructed for the auditory radiations, its reverse connections from A1-MGB, as well as the projections from A1-V1 and V1-A1. In all four of the measured tracts, the hemispheric asymmetries observed in the control group, were not found in participants who had undergone early monocular enucleation. Specifically, in the left auditory radiation and A1-MGB tracts, controls showed greater MD in the left compared to the right hemisphere, in addition to higher leftward AD. Increased average diffusivity associated with larger AD (and unchanged RD) can represent a variety of structural differences, such as improved fibre coherence or loss of neurofibrils (Kinoshita et al., 1999). The asymmetries reported here in the auditory radiations and A1-MGB connections have not previously been demonstrated in healthy individuals or other forms of sensory loss. However, the diffusion literature on the auditory radiations remains limited, and these differences may be the result of previous studies using considerably fewer diffusion directions that lacked the sensitivity necessary to reveal the hemispheric asymmetries found in the present study. The FA and MD values obtained in the present study for both groups of participants approximate those previously reported in the literature (Lutz et al., 2007; Roberts et al., 2009).

Comparison of the descriptive statistics between groups revealed that the asymmetries in AD and MD were not present in ME participants due to higher right, rather than lower left, hemisphere values. These marginal right hemisphere increases in AD and MD were not large

enough for any of the between groups comparisons to be significantly different, contrary to expectations. There remains limited DTI literature in which the control group exhibits significant hemispheric asymmetries that the patient, or otherwise specialised group of interest, does not. For example, in schizophrenic individuals, who do not show the significant FA asymmetries that controls do in structures throughout the brain, the absence of asymmetries has been attributed to variety of potential causes. Some of these include: functional disconnection, damage to the fibre tracts, other structural or functional differences, as well as increased interindividual variability in the measured parameters (Park et al., 2004). Interestingly, no investigation into potential auditory system changes has been made in early blind individuals (or other forms of vision loss) and similar absences of hemispheric asymmetries have not been reported in other white matter structures following vision loss (e.g., Shimony et al., 2006; Shu et al., 2009a; Shu et al., 2009b; Zhang et al., 2015). In the present study, a possible cause for the increase in AD is improved fibre coherence, which would also facilitate the higher MD levels reported. Increased fibre coherence in the right hemisphere of ME participants may reflect accommodation for the loss of one eye (Dubois et al., 2008; Takahashi et al., 2000). Although changes in AD alone cannot be taken to indicate changes in function (Jones et al., 2013), it is possible that the lack of asymmetries observed in ME participants support, in part, the enhanced auditory processing in this group (Hoover et al., 2012; Moro & Steeves, 2012; Moro & Steeves, 2013). Previous studies have also shown higher AD values following axonal injury or inflammation (Song et al., 2002), however, given that sensory input was lost from the visual modality only, and that audition is not negatively impacted in this group, degeneration of the auditory system is not expected. As with the visual system, the previously reported grey matter asymmetries in the MGB (Moro et al., 2015) and the supramarginal gyrus (Kelly et al., 2015) are not reflected in the structural white

matter differences in the auditory connections between the MGB and A1.

Analysis of diffusion parameters for the audiovisual tracts connecting A1 and V1 revealed a similar pattern of results as those for the auditory system. Left-higher-than-right asymmetries in MD and RD were found in the control group, but not the ME group, for both tracts. These asymmetries may reflect mechanisms such as lower axonal density, or increased fibre calibre, which facilitate diffusion in extra- and intra-axonal spaces, respectively (Schmierer et al., 2007). Given the presence of the MD and RD asymmetries in the control group, it may be that they are naturally occurring in these tracts in binocularly intact individuals. Due to the novelty of this connection, there is no previous research investigating the measured diffusion indices and so it cannot be said whether the present results replicate past findings. However, based on the seed and termination points used, these tracts add to the literature supporting the existence of these cortico-cortical tracts (Beer et al., 2011; Beer et al., 2013), in both an additional control group, as well as a patient group.

Higher right hemisphere values again appear to be the cause of the absent asymmetries in ME participants, with the increase in MD likely driven by the larger RD values. Thus, early monocular enucleation may have affected the normal development of these tracts to an extent that eliminated the hemispheric asymmetries but did not result in significant between groups differences. Although the novelty of this connection means its developmental trajectory is unknown, other long association fibres tend to myelinate later in life (Yakovlev & Lecours, 1967), making it quite possible that the development of these projections between A1 and V1 were influenced by the early loss of one eye. This is supported by additional results obtained from the reconstruction of the V1-A1 projections that were not significant in the A1-V1 projections. In the V1-A1 projections only, ME participants had significantly smaller FA values

compared to controls in the right hemisphere. A significant leftward asymmetry was also observed for AD in the ME group that appears to be the result of smaller right hemisphere values. It is probable that this simultaneous decrease in AD and increase in RD supported the decrease in FA in the ME group.

As all of these differences in ME participants appear to have occurred due to changes in the right hemisphere tract, it is possible that these are distal effects of the changes observed in the right optic radiation. Previously, it was speculated that the increased RD in the right optic radiation could have influenced the differences in V1-V1 projections beginning in the right hemisphere, which exhibited significantly lower FA. Thus, it can similarly be postulated that this difference may extend to the connections between A1 and V1. This could account for the higher rightward RD in these tracts, which eliminated the asymmetries observed in controls, as well as lowered the FA and in the right V1-A1 projections. If this influence of the visual pathway can be assumed, then the fact that a reduction in FA was not reported for the A1-V1 projections may indicate a distance effect, in which more distal portions of long fibres have a lower probability of being reconstructed using probabilistic tractography, such that the reduced FA values were not observed when tracking began in A1 (Mori & van Zijl, 2002; Tournier et al., 2011). This also assumes that the connections between A1 and V1 are reciprocal and that the reverse tractography from V1-A1 occurs through the same fibre bundle as when the tract is reconstructed from A1-V1, which is not necessarily the case. The additional leftward AD asymmetry in the V1-A1 connections, which was likely driven by the higher right hemisphere RD values (resulting in lower right hemisphere AD), may also have been subject to distance effects when reconstructed from A1-V1. Reduced FA and AD resulting from elevated RD due to the changes observed in the primary visual pathway would support the idea of immature fibre tracts from altered visual

input early in life, as both fibre coherence (AD) and organisation (FA) would be reduced as a consequence (Dubois et al., 2008; Takahashi et al., 2000). However, the observed reduction in AD does not support the hypothesis of transneuronal degeneration from lesions to the anterior visual system (i.e., from the surgical eye removal), as AD tends to increase with axonal pathology (Song et al., 2002). Of course, it is possible that an additional mechanism is operating on AD in this tract, such as increased fibre diameter (Budde et al., 2009; Jones et al., 2013; Song et al., 2003).

As with the other auditory and visual tracts that exhibited changes in ME participants, the connections between A1 and V1 are by and large maintained, and do not reflect the previously demonstrated structural changes to V1 or supramarginal gyrus (Kelly et al., 2015). While the preservation of this tract may enable normal multisensory integration following the early loss of one eye, it is likely that other structural or functional differences support the changes in multisensory processing observed in this group (Moro et al., 2014).

Other major white matter tracts

Of the 11 major white matter structures investigated, differences between participants who had undergone early monocular enucleation and binocularly intact controls were observed for three tracts. Consistent with hypotheses, two of these tracts have direct connections to the occipital lobe, namely the ILF, which connects the anterior temporal lobe to occipital cortex (including visual association areas) (Catani et al., 2003; Wakana et al., 2004), and the IFOF, with connections between the orbito-frontal, parietal, temporal, and occipital regions (Martino, Brogna, Robles, Vergani & Duffau, 2010). In both of these tracts, significant leftward asymmetries in AD, MD, and RD were found in control participants only. As changes were seen in both AD and RD, these asymmetries likely resulted from a combination of factors influencing

intra- and extra-axonal space (Le Bihan, 2003; Schmierer et al., 2007; Song et al., 2002). The average values for MD and FA (the only previously measured diffusion indices) for controls and ME participants fell within the anticipated range for both tracts based on previous reports. However, the observed hemispheric asymmetries in MD, AD, and RD have not previously been demonstrated, or investigated, and the nature of a potential FA asymmetry continues to be disputed (de Schotten et al., 2011; Lebel & Beaulieu, 2011; Park et al., 2004; Verhoeven et al., 2010; Wu, Sun, Wang & Wang, 2016).

The ILF was the only tract of the 11 additional structures investigated that showed a significant between groups difference. Significantly smaller values for FA were found in the right ILF of ME participants, suggesting microstructural differences compared to controls, which may be related to the lack of observed hemispheric asymmetries. In the ME group, higher RD in the right tract appears to be the main driving factor for the increase in MD (and subsequent absence of asymmetry) and the reduced FA in the same hemisphere. Recent research has provided evidence for maturation of the ILF, specifically its myelination, into the early thirties (Filley, 2012; Westlye et al., 2009); thus there is potential for its development to be affected by early monocular enucleation. Considerably greater reductions in FA in the ILF have been reported in participants with glaucoma and amblyopia, which were attributed to the partial loss of vision (Li et al., 2015; Zikou et al., 2012). As the ILF receives input from the ventral visual stream, morphological or functional changes in the visual system of ME participants may have impacted the development of the ILF resulting in reduced FA. The current pattern of results is consistent with axonal immaturity, however, as mentioned in the discussion of the visual system tracts, these results could also represent axonal degeneration (e.g., Boucard et al., 2016; Shu et al., 2009a). Similar to the right-to-left interhemispheric V1 connections and right A1-V1

projections, changes to the ILF may reflect transneuronal degeneration or immaturity that has extended from structures earlier in the visual system.

Due to its connections to visual association areas, in particular the ventral visual stream, the ILF is thought to be responsible for tasks related to object and face processing, discrimination, and memory (Ffytche, 2008; Fox, Iaria & Barton, 2008). Previous research has demonstrated mild deficits in face processing following early monocular enucleation (Kelly et al., 2012a). In control participants as well as children with autism spectrum disorder, lower FA in the right ILF has been correlated with poorer face recognition abilities (Koldewyn et al., 2014; Tavor et al., 2014). Although facial recognition per se is not altered in ME participants, the structural differences in the right ILF may have some relation to the changes in holistic face processing observed in this group, perhaps through the reduction in connectivity between key processing regions.

Despite their considerable spatial overlap, the IFOF does not show the same between groups difference in FA as the ILF; however, it is the only tract measured in this study that exhibits a significant eye-dependent difference. Average diffusivity (MD) is significantly higher ipsilesionally compared to contralesionally in the IFOF of ME participants. Although the IFOF shows similar results to the ILF in amblyopic participants, no significant eye-dependent effects have previously been reported (Li et al., 2015). The ipsilesional increase in MD may be a downstream effect of the enlarged ipsilesional V1 (Kelly et al., 2015). This could be due to functional changes to this region following the increased surface area and gyrification, or a related structural change extending from the altered V1. Larger MD values tend to indicate an increased presence of water that causes diffusion to occur more quickly, and can be the result of any of the factors that affect AD and/or RD (Beaulieu & Allen, 1994). The IFOF also passes

through the LGN (Kier, Staib, Davis & Bronen, 2004) which has been shown to be significantly larger ipsilesionally compared to contralesionally, despite showing an overall loss of volume relative to controls (Kelly et al., 2014). Therefore, it may be that the IFOF was influenced by the LGN as well as, or in place of, V1. However, as these eye-dependent grey matter changes do not appear to have affected any of the other related white matter structures investigated (e.g., the optic radiations or interhemispheric V1 projections), it remains unclear as to why the IFOF specifically was influenced by the eye removed, or whether there is a different mechanism at play. Overall, given the absence of between groups differences, the IFOF appears to remain intact following long-term survival from early monocular enucleation. Like the ILF, the IFOF is also associated with the ventral visual stream and its functions, being attributed to visual object identification and processing (Fox et al., 2008; Kikinis et al., 2013). As these processes are, to our knowledge, unchanged following early monocular enucleation, it is logical that there are no significant between groups differences, despite the inconsistencies in asymmetries.

Outside of those tracts directly connected to occipital cortex, ME participants also did not demonstrate the asymmetries exhibited by controls in the hippocampal portion of the cingulum. Similar to the ILF and IFOF, analysis of control participants' data for the hippocampus revealed significant leftward asymmetries in AD, MD, and RD that were not observed for the ME group. The values obtained for both groups were somewhat higher for FA and MD than those previously reported (Gong et al., 2005; Iaria, Lanyon, Fox, Giaschi & Barton, 2008; Lebel & Beaulieu, 2011); however, diffusion parameters for the hippocampus can vary in relation to certain behavioural abilities of the participants (Iaria et al., 2008). Past research has also provided conflicting reports of a rightward asymmetry in MD, as well as a leftward asymmetry in FA (Lebel & Beaulieu, 2011), neither of which were found in the present study.

That early monocular enucleation can have such widespread effects on white matter is somewhat surprising, although the hippocampus does have a clear dependence on visual information. In addition to supporting several autonomic nervous system functions and being a centre for emotion (Pinel, 2011), the hippocampus plays a role in visual memory (Lepage, Habib & Tulving, 1998) and spatial processing. It is also closely connected to the parahippocampal gyrus, which not only provides an indirect connection to visual cortex, but also contributes to scene processing itself (Epstein, 2008; Epstein & Kanwisher 1998; Epstein, Parker & Feiler, 2007). Thus altered visual input during development could affect the hippocampus in several ways. Once more, the absence of asymmetries appears to be the result of marginally higher AD, MD, and RD in the right hippocampus of ME participants. This now familiar pattern of results may again reflect axonal immaturity due to the reduced visual input early in life, or transneuronal degeneration that extended from other visual areas (e.g., Boucard et al., 2016; Shu et al., 2009a). Thus far, investigation into the effects of early visual deprivation on hippocampal development has been limited to changes in grey matter. In early blind individuals, changes were restricted to the right hippocampus, with hypertrophy occurring in the anterior portion and atrophy observed in the posterior segment (Chebat et al., 2007; Leporé et al., 2009; Leporé et al., 2010). On the other hand, increased right posterior hippocampal volume has been demonstrated in London taxi drivers with expert navigational skills and extensive experience (Maguire et al., 2010). These findings, together with the fact that the right posterior hippocampus is thought to support visuospatial memory, suggest that the atrophy of the posterior segment of the hippocampus in early blind participants is the result of reduced functional load and inexperience (Chebat et al., 2007; Leporé et al., 2009; Leporé et al., 2010). Although comparisons cannot necessarily be made between grey and white matter changes, the current results may reflect white matter

degeneration in the right hippocampus, which could be accounted for by the reduced visual memory demands. However, these findings must be interpreted in light of the fact that there were no significant differences between the ME group and the control group. Further research is required to clarify the influence of early vision loss on hippocampal development, particularly with regards to its white matter.

The SLF and the SLFt are among those tracts that showed no differences between groups, and while asymmetries in three of the four diffusion parameters are consistent in both participant groups, there is a single asymmetry that was not found in ME participants. Whereas the ILF is associated with the ventral visual stream, the SLF projects from the dorsal visual stream with connections extending to parietal, temporal, and frontal lobes (Catani et al., 2002). Among other functional roles, the SLF contributes to visuospatial functioning, particularly in the right hemisphere (Makris et al., 2005; Tuch et al., 2005). In individuals with Williams Syndrome, elevated FA in the right SLF correlates with deficits in visuospatial functioning (Hoeft et al., 2007). Given the intact performance on such tasks following early monocular enucleation, it is not surprising that there are no significant group differences, and for the most part, no variation in the presence of hemispheric asymmetries. However, ME participants do not show the leftward asymmetry in AD that is apparent in controls, although the average values in both hemispheres continue to be in the control range (Lebel & Beaulieu, 2011; Verhoeven et al., 2010). The asymmetry appears to have been reduced as a result of a small increase in AD in the right hemisphere of the ME group. An increase in AD can be representative of both axonal pathology and improved fibre coherence (Dubois et al., 2008; Song et al., 2002; Takahashi et al., 2000). In the case of a compensatory mechanism (e.g., better fibre coherence), it is possible that this slight increase may contribute to the enhanced visuospatial processing abilities in these individuals (see

Kelly et al., 2012b; Steeves et al., 2008 for review). However, without further information on this group, any association between white matter microstructure and functional changes is speculation.

The remainder of the major white matter tracts investigated showed no significant between groups differences or inconsistencies in the presence (or absence) of asymmetries across groups. These tracts consisted of the cingulate gyrus, the uncinate fasciculus, the ATR, the corticospinal tract, and the forceps, both major and minor. Excluding the forceps major, none of these tracts are directly connected to visual regions, although the ATR and corticospinal tract do receive indirect visual input (Manford & Andermann, 1998; Yu et al., 2007). Therefore, it is not unexpected that these tracts remain unchanged in ME participants, particularly as research in other forms of partial vision loss provides no indication of global grey matter or functional differences that might suggest significant alterations in these distant, arguably unrelated tracts (e.g., Li et al., 2015; Michelson et al., 2013; Xie et al., 2007). Early monocular enucleation however, has been shown to significantly increase global surface area and gyrification of grey matter relative to controls (Kelly et al., 2015). Accordingly, although there is no evidence for changes based on the diffusion indices of the specified tracts, future work should examine global white matter volume to assess if there are any differences in relation to the change in grey matter. Overall, the diffusion values obtained for these tracts are consistent with past research. However, the relevant presence or absence of asymmetries is not firmly established in any of these structures and thus correspondence with the literature is variable across tracts (de Schotten et al., 2011; Lebel & Beaulieu, 2011; Verhoeven et al., 2010).

Conclusions

Understanding how the brain develops and how it changes in response to the environment

is fundamental to neuroplasticity. Neuroimaging in individuals who have undergone early monocular enucleation has provided evidence for morphological adaptations in adult cortical and subcortical visual, auditory, and multisensory regions (Kelly et al., 2015; Kelly et al., 2014; Moro et al., 2015). This study is the first to investigate the long-term changes to white matter structure following partial vision loss from early monocular enucleation. Through the use of DTI and probabilistic tractography, we report findings of structural white matter differences in ME participants that extend beyond the primary visual pathway to include interhemispheric, auditory, and multisensory tracts, as well as several visually-dependent long association fibres.

Contrary to hypotheses, the structural connectivity differences observed in ME participants do not reflect the changes to cortical and subcortical grey matter previously reported in this group (Kelly et al., 2015; Kelly et al., 2014; Moro et al., 2015). Independent of eye of enucleation the present results demonstrate changes in diffusion parameters exclusively in the right hemisphere. Two broad patterns of results were apparent: 1) significantly higher RD compared to controls in the right optic radiation, apparently resulting in associated decreases in FA in the right interhemispheric, multisensory, and ILF connections, and 2) an absence of asymmetries due to elevated right hemisphere values in the optic radiations, auditory tracts, audiovisual tracts, and several major white matter structures (ILF, IFOF, SLF, SLFt, hippocampus). Overall our results suggest widespread neuroplasticity in the white matter structure of adults who have undergone early monocular enucleation. Despite the minor structural differences reported, all of the fibre tracts measured remain largely intact following early monocular enucleation. This supports the premise previously put forward that different forms of accommodation occur following the complete removal of one eye, compared to other types of partial visual deprivation in which degraded visual input continues to reach the brain

(e.g., Kelly et al., 2015; Michelson et al., 2013).

The primary mechanisms proposed here to account for the reported structural differences were transneuronal degeneration and axonal immaturity, except in the case of the auditory system tracts in which increased fibre coherence was suggested. Transneuronal degeneration was argued to have stemmed from lesions to the optic nerve following removal of the eye (e.g., Shu et al., 2009a), whereas axonal immaturity was attributed to reduced activity in the visual pathway (e.g., Boucard et al., 2016). Neither of these mechanisms, however, can account for the changes being limited to the right hemisphere. It is difficult to present possible explanations for these asymmetrical effects of enucleation, as we cannot be certain of the structural changes the diffusion indices represent (Jones et al., 2013). For example, axonal immaturity may be the consequence of reduced functional load in the right hemisphere for certain visual functions. The right hemisphere is thought to be specialised for visuospatial functioning (Filley, 2012) while right lateralisation of visual memory and face processing has also been demonstrated (e.g., Chebat et al., 2007; Fox et al., 2008). The 50% reduction in visual input to the brain following early monocular enucleation may have decreased the processing demands in these regions resulting in immature fibre bundles. However, if this were the case, it is unclear whether the reported behavioural changes were the cause or effect of the structural white matter changes. Moreover, the right hemisphere also tends to have a higher volume of white matter compared to the left hemisphere (Hellige, 1993). This may make white matter structures in the right hemisphere more susceptible to the effects of early monocular enucleation.

Visual activity may likewise contribute to the overall maintenance of white matter tracts observed in ME participants (e.g., Barb et al., 2011). As any functional changes following early monocular enucleation are as of yet unknown, it is equally likely that visual activity remains

sufficient to support normal maturation of white matter, as it is that activity is inadequate and results in axonal immaturity. It is also possible that, despite not reflecting the eye-dependent asymmetries, white matter structure is preserved through the relatively intact cortical and subcortical regions (e.g., LGN, MGB, V1) (Kelly et al., 2015; Kelly et al., 2014; Moro et al., 2015). Although there is no evidence that these grey matter changes are related to function in ME participants, the somewhat normal size of these structures may support the visual activity required to maintain intact white matter. Similarly, the absence of grey matter atrophy, outside of the LGN, could be important for providing the target space needed for axon survival during development. It has previously been demonstrated that larger cortical areas can support denser networks of fibre bundles due to the increased volume of cortex (Putnam et al., 2009; Saron, Foxe, Simpson & Vaughan, 2003). Had significant atrophy occurred in these cortical regions following early monocular enucleation, the reduced target area for axons may have resulted in extensive degeneration and overall more severe changes in white matter development. Thus, the preservation of white matter structure in ME participants could be supported in a number of ways.

The current findings contribute to our understanding of the morphological adaptations underlying the behavioural changes reported in individuals who have undergone early monocular enucleation (Kelly et al., 2012; Steeves et al., 2008). These results indicate that changes occur to white matter as well as grey matter following early monocular enucleation, but that the alterations to structural connectivity do not reflect the observed differences in grey matter (e.g., Kelly et al., 2014). This disassociation suggests early visual deprivation has different effects on white and grey matter structures that may be the result of separate mechanisms of neuroplasticity. Overall, the global preservation of white matter in ME participants suggests that

it plays an important role in maintaining intact visual functioning in this group. The lack of asymmetries in the auditory system tracts may reflect adaptive compensation for the loss of one eye in this modality, consistent with previous behavioural findings in this group (e.g., Hoover et al., 2012). The differences in white matter changes in ME participants compared to other forms of monocular visual deprivation reaffirm that the complete removal of one eye has more compensatory effects than other types of partial vision loss (e.g., Boucard et al., 2016). The findings of this study will help expand our knowledge of neuroplasticity following altered sensory input early in life, serving as a model for other forms of partial sensory deprivation.

Limitations

DTI is valuable as one of the few non-invasive neuroimaging techniques for visualising white matter structure *in vivo*; however, as a relatively new methodology, it has a number of attendant limitations that all DTI studies share. These limitations are largely the result of a combination of the assumptions underlying DTI and our incomplete understanding of what precisely diffusion indices measure. First, all diffusion studies operate under the assumption of a Gaussian distribution for diffusion; that is, that there is a single dominant fibre orientation for each voxel, which is represented by the principal eigenvector (also known as AD). This is related to the second assumption that a single diffusion tensor model per voxel is sufficient to characterise the underlying microstructure (Jones, 2008). Based on the complex nature of white matter throughout brain, it has been proposed that as many as 90% of all voxels will host multiple fibre populations. Thus, in any given study, neither of the assumptions on which DTI is based are fulfilled (Jones et al., 2013). The result is an oversimplified diffusion tensor that is less than adequate for completely characterising white matter microstructure. This in turn causes issues such as the partial volume effect, wherein voxels in between two discrete tracts are given

an angle that is the average of the two, as well as difficulty resolving crossing or branching fibres (Jones et al., 2013; Mori, 2007). The latter concern is particularly relevant for the present study, which reconstructed the auditory radiations. The auditory radiations are relatively small tracts that cross the much larger ILF. This often results in issues performing tractography due to the crossing fibres (Berman et al., 2013). To ensure accuracy of the reconstruction, processing techniques that account for crossing fibres were used, namely BEDPOSTX and PROBTRACKX (Behrens et al., 2007; Behrens et al., 2003). However, both partial volume effects and crossing fibres can considerably influence FA, AD, and RD; therefore, it cannot strictly be said that changes in diffusion parameters represent microstructural differences in white matter (Jbabdi, Beherns & Smith, 2010). This is related to the issue of interpreting DTI results.

The conclusions that can be drawn from DTI results, in particular diffusion indices, are subject to their own limitations. In part, these can be attributed to the discordance between the scale at which diffusion-weighted data is collected (typically 2-3 mm) and the scale of axons (as small as 0.2 μm in diameter). As a result, the microscopic information at the level of the axon is averaged over the larger voxel volume (O'Donnell & Westin, 2011). In the case of high FA, it is required that there be both anisotropic diffusion at the cellular level, as well as homogeneous macrostructural components throughout the voxel (Mori & Zhang, 2006). It is this requirement that relates to the issue of crossing fibres and FA. Therefore, while diffusion indices are defined as measuring microstructural properties, they necessarily also reflect the macrostructure (i.e., at the voxel level) of white matter. This makes it difficult to say with certainty, what exactly each of the diffusion parameters measure. The most robust way of determining what structural changes the diffusion parameters represent is through post-mortem analysis, particularly in animal studies where influential factors such as myelin can be artificially manipulated. Even still,

it is difficult to make causal conclusions and changes are likely to vary across participant groups (e.g., Song et al., 2002). Thus, the interpretation of DTI data is limited in the certainty with which conclusions can be drawn regarding macro- and microstructural changes (Jones et al., 2013). The current study however benefits from the fact that comparisons were made between a clinical sample and a control group. This provides some assurance that the observed differences between groups truly indicate changes in white matter, although it does not help in confirming the nature of the structural change.

There are also study-specific limitations that must be addressed. First, the sample size used in the present study was relatively small, although it is within the limits of sample sizes typically used in neuroimaging studies with a patient group (e.g., Ciccarelli et al., 2005; Bridge et al., 2009; Guerreiro, Erfort, Henssler, Putzar & Röder, 2015; Shimony et al., 2006). This however, may have reduced the power, obscuring potentially significant differences between groups. This is compounded with the higher variability that is often reported in white matter in clinical groups (e.g., Park et al., 2004) as well as the inclusion of both left and right eye enucleated participants, both of which could have led to either false positives or negatives. To address this, effect sizes were calculated for all comparisons to obtain a measure of the magnitude of the difference. All of the reported results had large effect sizes providing confidence that they reflect true differences in white matter structure between groups. However, several results that did not reach significance after correcting for multiple comparisons had similarly large effect sizes, suggesting that the current results may be further clarified with a bigger sample size.

With regards to the DTI analyses, it can be argued the use of masks extracted from atlases (Desikan et al., 2006; Eickhoff et al., 2005; Mori et al., 2005) may not have provided the

most accurate representations of the location and size of brain structures, particularly in ME participants who demonstrate significant structural changes (Kelly et al., 2015; Kelly et al., 2014). Atlas-extracted masks were used as proton density scans were not available for all participants and functional data has not previously been collected in this group. However, both the size and location of these masks were assessed, and altered as needed, for all participants, and no further processing was conducted until we were confident that the masks were appropriate for each individual. A number of previous studies have also used masks from these atlases with success (e.g., Kantarci et al., 2010; Karnath, Rorden & Ticini, 2009; Revill, Namy, DeFife & Nygaard, 2014).

The nature of DTI is also limited in its inability to discern the direction of diffusion or functional activity (i.e., feedforward or feedback). In this study, seed-termination mask pairings were generated in both directions (e.g., MGB-A1 and A1-MGB). Given the differences in results between the two reconstructions, the findings were discussed as if for two separate tracts. However, the presence of unique feedback fibre bundles has not been confirmed for any of the tracts investigated and thus it may have been inappropriate to discuss the findings under this assumption. This also raises the issue of distance effects (Mori & van Zijl, 2002) as a number of long fibre bundles were investigated. It is possible that the mechanism causing the change in diffusion parameters was closer to the seed or termination mask, such that when the opposite reconstruction was performed the differences did not reach significance due to the lower probability of fibres being tracked at further distances from the seed point. Although the pattern of results between seed-termination and termination-seed tracts does not appear to indicate this, it may have been better practise to discuss these tracts as a single structure, reporting only those results that were significant in both reconstructions. Nevertheless, given the novelty of the

current study, and the fact that it would be premature to conclude that ME participants do not have additional fibre bundles beyond those of controls, the results of this study were discussed in such as way as to provide the most comprehensive review of the findings.

Future directions

Overall, the results from this study point to the importance of investigating potential functional differences in individuals who have undergone early monocular enucleation. In addition to contributing to our understanding of the behavioural differences following early monocular enucleation, fMRI data could help clarify the morphological changes demonstrated in this group. This is particularly true for the white matter findings reported here as, contrary to hypotheses, the differences found did not reflect the previously established changes in grey matter (Kelly et al., 2015; Kelly et al., 2014; Moro et al., 2015). In early deaf individuals, functional reorganisation has been presented as a potential cause for changes observed in frontal and temporal white matter (Kim et al., 2009). This is in contrast to research following early blindness in which white matter changes are almost strictly attributed to axonal degeneration or immaturity from lack of visual experience (e.g., Shimony et al., 2006; Shu et al., 2009a). Changes in the functional use of cortical and subcortical regions in ME participants may better reflect the observed white matter changes, and should be investigated in future work. In addition to assessing overall changes in functional activity in ME participants, functional connectivity analyses may also provide insight. Research in early blind individuals has revealed significant differences in functional connectivity between visual and other regions (e.g., frontal, somatosensory) (Liu et al., 2007; Wittenberg, Werhahn, Wassermann, Herscovitch & Cohen, 2004; Yu et al., 2008) that have not been shown to have altered structural connectivity (Shimony et al., 2006). These changes may support the intact structural connections in early blind

participants, or contribute to the associated behavioural changes (Liu et al., 2007; Wittenberg et al., 2004; Yu et al., 2008). Future research into functional connectivity in ME participants may help elucidate the findings reported here or present an alternative account for the behavioural differences in this group.

The acquisition of functional data would also be useful in future studies investigating white matter in ME participants. Functional data would allow for individualised functionally defined region of interest masks to be created and used in place of the atlas masks used in the current study. Potential changes in functional activity could also be used to inform which white matter structures to further examine. Future investigations into white matter structure should use diffusion spectrum imaging (DSI) or high angular resolution diffusion imaging (HARDI) in order to maximise spatial resolution, account for non-Gaussian diffusion processes, and better resolve crossing fibres (Descoteaux, Deriche, Knosche & Anwander, 2009). Ideally future studies would also be able to recruit more participants so that correlations could be performed between the diffusion indices and behavioural data in order to determine whether the observed structural changes can be considered 'adaptive'. Previous research in glaucoma patients revealed a significant positive correlation between FA in the optic radiations and visual acuity (Michelson et al., 2013). Given the largely intact white matter structure, and relatively unaltered visual behaviour following early monocular enucleation (Kelly et al., 2012b; Steeves et al., 2008), an investigation into potential correlations may prove interesting. Lastly, white matter volume was not assessed in this study. Extraction of white matter volumes and parcelation from neighbouring grey matter may provide findings that help explain the mechanisms underlying the structural white matter changes. A global assessment of white matter volume might also be insightful, as global increases in grey matter surface area and gyrification have previously been reported in

ME participants (Kelly et al., 2015).

Finally, magnetic resonance spectroscopy (MRS), a non-invasive method for assessing the biochemical and metabolite prevalence in the brain (Ross & Bluml, 2001), would also be an interesting and informative topic of study for future work as a tool for evaluating the neural activity and plasticity mechanisms underlying the structural changes that follow early monocular enucleation. MRS in early blind participants has revealed elevated myo-inositol in occipital cortex suggesting an increased proliferation or size of glial cells, and contributing to the understanding of functional changes and neuroplasticity following early blindness (Bernabeu, Alfaro, García & Fernández, 2009). Assessment of brain metabolites in occipital or temporal regions in ME participants may reveal findings that can be used to advance our understanding of functional and morphological changes in these individuals. Overall, future research that uses a combination of several neuroimaging techniques will help us move towards a more accurate global representation of the changes that occur both structurally and functionally following early monocular enucleation. This in turn will inform our more general understanding of neuroplasticity following altered sensory input early in life and neural development on the whole.

REFERENCES

Alais, D. & Burr D. (2004). The ventriloquist effect results from near-optimal bimodal integration. *Current Biology, 14*(3), 257-262.

Alais, D., Newell, F. N., & Mamassian, P. (2010). Multisensory processing in review: from physiology to behaviour. *Seeing and Perceiving, 23*(1), 3-38.

Alix, J. J. & Domingues, A. M. (2011). White matter synapses: form, function, and dysfunction. *Neurology*, *76*(4), 397-404.

Andersson, J. L., Jenkinson, M., & Smith, S. (2007a). Non-linear optimisation FMRIB technical report TR07JA1. *FMRIB Analysis Group of the University of Oxford*.

Andersson, J. L., Jenkinson, M., & Smith, S. (2007b). Non-linear registration, aka Spatial normalisation FMRIB technical report TR07JA2. *FMRIB Analysis Group of the University of Oxford*.

Barb, S. M., Rodriguez-Galindo, C., Wilson, M. W., Phillips, N. S., Zou, P., Scoggins, M. A., ... & Haik, B. G. (2011). Functional neuroimaging to characterize visual system development in children with retinoblastoma. *Investigative Ophthalmology & Visual Science*, *52*(5), 2619-2626.

Barnea-Goraly, N., Menon, V., Eckert, M., Tamm, L., Bammer, R., Karchemskiy, A., ... & Reiss, A. L. (2005). White matter development during childhood and adolescence: a cross-sectional diffusion tensor imaging study. *Cerebral Cortex*, *15*(12), 1848-1854.

Bartlett, E. L. (2013). The organization and physiology of the auditory thalamus and its processing acoustic features important for speech perception. *Brain & Language, 129*(1), 29-48.

Bavelier, D. & Neville, H. J. (2002). Cross-modal plasticity: where and how? *Nature Reviews*

Neuroscience, *3*(6), 443-452.

Beatty, R. M., Sadun, A. A., Smith, L., Vonsattel, J. P., & Richardson Jr., E. P. (1982). Direct demonstration of transsynaptic degeneration in the human visual system: a comparison of retrograde and anterograde changes. *Journal of Neurology, Neurosurgery and Psychiatry*, *45*(2)*,* 143-146.

Beaulieu, C. & Allen, P. S. (1994). Determinants of anisotropic water diffusion in nerves. *Magnetic Resonance in Medicine*, *31*(4), 394-400.

Beer, A. L., Plank, T., & Greenlee, M. W. (2011). Diffusion tensor imaging shows white matter tracts between human auditory and visual cortex. *Experimental Brain Research*, *213*(2-3), 299-308.

Beer, A. L., Plank, T., Meyer, G., & Greenlee, M. W. (2013). Combined diffusion-weighted and functional magnetic resonance imaging reveals a temporal-occipital network involved in auditory-visual object processing. *Frontiers in Integrative Neuroscience*, *7*(5), 0-5.

Behrens, T. E. J., Johansen-Berg, H., Jbabdi, S., Rushworth, M. F. S., & Woolrich, M. W. (2007). Probabilistic diffusion tractography with multiple fibre orientations: what can we gain? *Neuroimage*, *34*(1), 144-155.

Behrens, T. E. J., Woolrich, M. W., Jenkinson, M., Johansen-Berg, H., Nunes, R. G., Clare, S., ... & Smith, S. M. (2003). Characterization and propagation of uncertainty in diffusion-weighted MR imaging. *Magnetic Resonance in Medicine*, *50*(5), 1077-1088.

Berman, J. I., Lanza, M. R., Blaskey, L., Edgar, J. C., & Roberts, T. P. (2013). High angular resolution diffusion imaging probabilistic tractography of the auditory radiation. *American Journal of Neuroradiology*, *34*(8), 1573-1578.

Bernabeu, A., Alfaro, A., García, M., & Fernández, E. (2009). Proton magnetic resonance

spectroscopy (1 H-MRS) reveals the presence of elevated myo-inositol in the occipital cortex of blind subjects. *Neuroimage*, *47*(4), 1172-1176.

Bertelson, P. & Aschersleben G. (1998). Automatic visual bias of perceived auditory location. *Psychonomic Bulletin & Review, 5*(3)*,* 482-489.

Boucard, C. C., Hanekamp, S., Ćurčić-Blake, B., Ida, M., Yoshida, M., & Cornelissen, F. W. (2016). Neurodegeneration beyond the primary visual pathways in a population with a high incidence of normal-pressure glaucoma. *Ophthalmic and Physiological Optics*, *36*(3), 344-353.

Bowns, L., Kirshner, E. L., & Steinbach, M. J. (1994). Shear sensitivity in normal and monocularly enucleated adults. *Vision Research*, *34*(24), 3389-3395.

Bridge, H., Cowey, A., Ragge, N., & Watkins, K. (2009). Imaging studies in congenital anophthalmia reveal preservation of brain architecture in 'visual' cortex. *Brain*, *132*(12), 3467-3480.

Brown, H. D., Woodall, R. L., Kitching, R. E., Baseler, H. A., & Morland, A. B. (2016). Using magnetic resonance imaging to assess visual deficits: a review. *Ophthalmic and Physiological Optics*, *36*(3), 240-265.

Budde, M. D., Xie, M., Cross, A. H., & Song, S. K. (2009). Axial diffusivity is the primary correlate of axonal injury in the experimental autoimmune encephalomyelitis spinal cord: a quantitative pixelwise analysis. *The Journal of Neuroscience*, *29*(9), 2805-2813.

Catani, M. & de Schotten, M. T. (2008). A diffusion tensor imaging tractography atlas for virtual in vivo dissections. *Cortex*, *44*(8), 1105-1132.

Catani, M., Howard, R. J., Pajevic, S., & Jones, D. K. (2002). Virtual in vivo interactive dissection of white matter fasciculi in the human brain. *Neuroimage*, *17*(1), 77-94.

Catani, M., Jones, D. K., Donato, R., & Ffytche, D. H. (2003). Occipito-temporal connections in the human brain. *Brain*, *126*(9), 2093-2107.

Ciccarelli, O., Toosy, A. T., Hickman, S. J., Parker, G. J., Wheeler-Kingshott, C. A., Miller, D. H., & Thompson, A. J. (2005). Optic radiation changes after optic neuritis detected by tractography-based group mapping. *Human Brain Mapping*, *25*(3), 308-316.

Chebat, D. R., Chen, J. K., Schneider, F., Ptito, A., Kupers, R., & Ptito, M. (2007). Alterations in right posterior hippocampus in early blind individuals. *Neuroreport*, *18*(4), 329-333.

Colavita, F. B. (1974). Human sensory dominance. *Perception and Psychophysics, 16*(2), 409-412.

Colavita, F. B. & Weisberg, D. (1979). A further investigation of visual dominance. *Perception & Psychophysics, 25*(4), 345-347.

Dayan, M., Munoz, M., Jentschke, S., Chadwick, M. J., Cooper, J. M., Riney, K., ... & Clark, C. A. (2015). Optic radiation structure and anatomy in the normally developing brain determined using diffusion MRI and tractography. *Brain Structure and Function*, *220*(1), 291-306.

de Schotten, M. T., Bizzi, A., Dell'Acqua, F., Allin, M., Walshe, M., Murray, R., ... & Catani, M. (2011). Atlasing location, asymmetry and inter-subject variability of white matter tracts in the human brain with MR diffusion tractography. *Neuroimage*, *54*(1), 49-59.

Descoteaux, M., Deriche, R., Knosche, T. R., & Anwander, A. (2009). Deterministic and probabilistic tractography based on complex fibre orientation distributions. *IEEE Transactions on Medical Imaging*, *28*(2), 269-286.

Desikan, R. S., Ségonne, F., Fischl, B., Quinn, B. T., Dickerson, B. C., Blacker, D., ... & Albert, M. S. (2006). An automated labeling system for subdividing the human cerebral cortex

on MRI scans into gyral based regions of interest. *Neuroimage*, *31*(3), 968-980.

Dougherty, R. F., Ben-Shachar, M., Bammer, R., Brewer, A. A., & Wandell, B. A. (2005). Functional organization of human occipital-callosal fiber tracts. *Proceedings of the National Academy of Sciences of the United States of America*, *102*(20), 7350-7355.

Dubois, J., Dehaene-Lambertz, G., Soarès, C., Cointepas, Y., Le Bihan, D., & Hertz-Pannier, L. (2008). Microstructural correlates of infant functional development: example of the visual pathways. *The Journal of Neuroscience*, *28*(8), 1943-1948.

Egeth, H. E. & Sager, L. C. (1977). On the Locus of Visual Dominance. *Perception and Psychophysics, 22*(1), 77-86.

Eickhoff, S. B., Heim, S., Zilles, K., & Amunts, K. (2006). Testing anatomically specified hypotheses in functional imaging using cytoarchitectonic maps. *Neuroimage*, *32*(2), 570-582.

Eickhoff, S. B., Paus, T., Caspers, S., Grosbras, M. H., Evans, A. C., Zilles, K., & Amunts, K. (2007). Assignment of functional activations to probabilistic cytoarchitectonic areas revisited. *Neuroimage*, *36*(3), 511-521.

Eickhoff, S. B., Stephan, K. E., Mohlberg, H., Grefkes, C., Fink, G. R., Amunts, K., & Zilles, K. (2005). A new SPM toolbox for combining probabilistic cytoarchitectonic maps and functional imaging data. *Neuroimage*, *25*(4), 1325-1335.

Epstein, R. A. (2008). Parahippocampal and retrosplenial contributions to human spatial navigation. *Trends in Cognitive Sciences*, *12*(10), 388-396.

Epstein, R. & Kanwisher, N. (1998). A cortical representation of the local visual environment. *Nature*, *392*(6676), 598-601.

Epstein, R. A., Parker, W. E., & Feiler, A. M. (2007). Where am I now? Distinct roles for

parahippocampal and retrosplenial cortices in place recognition. *The Journal of Neuroscience*, *27*(23), 6141-6149.

Ffytche, D. H. (2008). The hodology of hallucinations. *Cortex*, *44*(8), 1067-1083.

Filler, A. G., Tsuruda, J. S., Richards, T. L., & Howe, F. A. (1992). Images, apparatus, algorithms and methods. *UK Patent Office GB9210810*.

Filley, C. M. (2012). *The behavioral neurology of white matter* (2nd ed.). Oxford, UK: Oxford University Press.

Fox, C. J., Iaria, G., & Barton, J. J. (2008). Disconnection in prosopagnosia and face processing. *Cortex*, *44*(8), 996-1009.

Frazier, J. A., Chiu, S., Breeze, J. L., Makris, N., Lange, N., Kennedy, D. N., ... & Hodge, S. M. (2005). Structural brain magnetic resonance imaging of limbic and thalamic volumes in pediatric bipolar disorder. *American Journal of Psychiatry*, *162*(7), 1256-1265.

Freeman, R. D. & Bradley, A. (1980). Monocularly deprived humans: nondeprived eye has supernormal vernier acuity. *Journal of Neurophysiology*, *43*(6), 1645-1653.

Gao, W., Lin, W., Chen, Y., Gerig, G., Smith, J. K., Jewells, V., & Gilmore, J. H. (2009). Temporal and spatial development of axonal maturation and myelination of white matter in the developing brain. *American Journal of Neuroradiology*, *30*(2), 290-296.

Garey, L. J. & De Courten, C. (1983). Structural development of the lateral geniculate nucleus and visual cortex in monkey and man. *Behavioural Brain Research*, *10*(1), 3-13.

Godement, P., Saillour, P., & Imbert, M. (1980). The ipsilateral optic pathway to the dorsal lateral geniculate nucleus and superior colliculus in mice with prenatal or postnatal loss of one eye. *Journal of Comparative Neurology*, *190*(4), 611-626.

Godement, P., Salaün, J., & Métin, C. (1987). Fate of uncrossed retinal projections following

early or late prenatal monocular enucleation in the mouse. *Journal of Comparative Neurology*, *255*(1), 97-109.

Goldby, F. (1957). A note on transneuronal atrophy in the human lateral geniculate body. *Journal of Neurology, Neurosurgery and Psychiatry*, *20*(3), 202-207.

Goldstein, J. M., Seidman, L. J., Makris, N., Ahern, T., O'Brien, L. M., Caviness, V. S., ... & Tsuang, M. T. (2007). Hypothalamic abnormalities in schizophrenia: sex effects and genetic vulnerability. *Biological Psychiatry*, *61*(8), 935-945.

Gong, G., Jiang, T., Zhu, C., Zang, Y., Wang, F., Xie, S., ... & Guo, X. (2005). Asymmetry analysis of cingulum based on scale-invariant parameterization by diffusion tensor imaging. *Human Brain Mapping*, *24*(2), 92-98.

González, E. G., Lillakas, L., Greenwald, N., Gallie, B. L., & Steinbach, M. J. (2014). Unaffected smooth pursuit but impaired motion perception in monocularly enucleated observers. *Vision Research*, *101*, 151-157.

González, E. G., Lillakas, L., Lam, A., Gallie, B. L., & Steinbach, M. J. (2013). Horizontal saccade dynamics after childhood monocular enucleation horizontal saccades of enucleated observers. *Investigative Ophthalmology & Visual Science*, *54*(10), 6463-6471.

González, E. G., Steeves, J. K. E., Kraft, S. P., Gallie, B. L., & Steinbach, M. J. (2002). Foveal and eccentric acuity in one-eyed observers. *Behavioural Brain Research, 128*(1), 71-80.

Grigonis, A. M., Pearson, H. E., & Murphy, E. H. (1986). The effects of neonatal monocular enucleation on the organization of ipsilateral and contralateral retinothalamic projections in the rabbit. *Developmental Brain Research*, *29*(1), 9-19.

Guerreiro, M. J., Erfort, M. V., Henssler, J., Putzar, L., & Röder, B. (2015). Increased visual

cortical thickness in sight-recovery individuals. *Human Brain Mapping*, *36*(12), 5265-5274.

Guzzetta, A., D'Acunto, G., Rose, S., Tinelli, F., Boyd, R., & Cioni, G. (2010). Plasticity of the visual system after early brain damage. *Developmental Medicine and Child Neurology, 52*(10)*,* 891-900.

Hellige, J. B. (1993). *Hemispheric asymmetry: what's right and what's left*. S. M. Kosslyn (Ed.). Cambridge, MA: Harvard University Press

Hickey, T. & Guillery, R. (1979). Variability of laminar patterns in the human lateral geniculate nucleus. *Journal of Comparative Neurology*, *183*(2), 221-246.

Hilgetag, C. C. & Barbas, H. (2006). Role of mechanical factors in the morphology of the primate cerebral cortex. *PLoS Computer Biology*, *2*(3), e22.

Hoeft, F., Barnea-Goraly, N., Haas, B. W., Golarai, G., Ng, D., Mills, D., ... & Reiss, A. L. (2007). More is not always better: increased fractional anisotropy of superior longitudinal fasciculus associated with poor visuospatial abilities in Williams syndrome. *The Journal of Neuroscience*, *27*(44), 11960-11965.

Hofer, S., Karaus, A., & Frahm, J. (2010). Reconstruction and dissection of the entire human visual pathway using diffusion tensor MRI. *Frontiers in Neuroanatomy*, *4*, 1-15.

Hoover, A. E. N., Harris, L. R., & Steeves, J. K. E. (2012). Sensory compensation in sound localization in people with one eye. *Experimental Brain Research, 216*(4), 565-74.

Horton, J. C. (1997). Wilbrand's knee of the primate optic chiasm is an artefact of monocular enucleation. *Transactions of the American Ophthalmological Society*, *95*, 579-609.

Horton, J. C. & Hocking, D. R. (1998). Effect of early monocular enucleation upon ocular

dominance columns and cytochrome oxidase activity in monkey and human visual cortex. *Visual Neuroscience*, *15*(2), 289-303.

Hsiao, K. (1984). Bilateral branching contributes minimally to the enhanced ipsilateral projection in monocular Syrian golden hamsters. *The Journal of Neuroscience*, *4*(2), 368-373.

Hua, K., Zhang, J., Wakana, S., Jiang, H., Li, X., Reich, D. S., ... & Mori, S. (2008). Tract probability maps in stereotaxic spaces: analyses of white matter anatomy and tract specific quantification. *Neuroimage*, *39*(1), 336-347.

Huttenlocher, P. R. & De Courten, C. (1986). The development of synapses in striate cortex of man. *Human Neurobiology*, *6*(1), 1-9.

Iaria, G., Lanyon, L. J., Fox, C. J., Giaschi, D., & Barton, J. J. (2008). Navigational skills correlate with hippocampal fractional anisotropy in humans. *Hippocampus*, *18*(4), 335-339.

Javad, F., Warren, J. D., Micallef, C., Thornton, J. S., Golay, X., Yousry, T., & Mancini, L. (2014). Auditory tracts identified with combined fMRI and diffusion tractography. *Neuroimage*, *84*, 562-574.

Jbabdi, S., Behrens, T. E., & Smith, S. M. (2010). Crossing fibres in tract-based spatial statistics. *Neuroimage*, *49*(1), 249-256.

Jefferey, G. (1984). Transneuronal effects of early eye removal on geniculo-cortical projection cells. *Developmental Brain Research*, *13*(2), 257-263.

Jenkinson, M., Bannister, P., Brady, M., & Smith, S. (2002). Improved optimization for the robust and accurate linear registration and motion correction of brain images. *Neuroimage*, *17*(2), 825-841.

Jenkinson, M., Beckmann, C. F., Behrens, T. E., Woolrich, M. W., & Smith, S. M. (2012). Fsl.

Neuroimage, *62*(2), 782-790.

Jenkinson, M. & Smith, S. (2001). A global optimisation method for robust affine registration of brain images. *Medical Image Analysis*, *5*(2), 143-156.

Jones, D. K. (2008). Studying connections in the living human brain with diffusion MRI. *Cortex*, *44*(8), 936-952.

Jones, D. K., Knösche, T. R., & Turner, R. (2013). White matter integrity, fiber count, and other fallacies: the do's and don'ts of diffusion MRI. *Neuroimage*, *73*, 239-254.

Kantarci, K., Avula, R., Senjem, M. L., Samikoglu, A. R., Zhang, B., Weigand, S. D., ... & Ferman, T. J. (2010). Dementia with Lewy bodies and Alzheimer disease neurodegenerative patterns characterized by DTI. *Neurology*, *74*(22), 1814-1821.

Karnath, H. O., Rorden, C., & Ticini, L. F. (2009). Damage to white matter fiber tracts in acute spatial neglect. *Cerebral Cortex*, *19*(10), 2331-2337.

Kelly, K. R., DeSimone, K. D., Gallie, B. L., & Steeves, J. K. E. (2015). Increased cortical surface area and gyrification following long-term survival from early monocular enucleation. *Neuroimage: Clinical, 7*, 297-305.

Kelly, K. R., Gallie, B. L., & Steeves, J. K. E. (2012a). Impaired face processing in early monocular deprivation from enucleation. *Optometry and Vision Science, 89*(2)*,* 137-47.

Kelly, K. R., McKetton, L., Schneider, K. A., Gallie, B. L., & Steeves, J. K. E. (2014). Altered anterior visual system development following early monocular enucleation. *Neuroimage: Clinical*, *4*, 72-81.

Kelly, K. R., Moro, S. S., & Steeves, J. K. E. (2012b). Living with one eye: Plasticity in visual and auditory systems. In J.K.E. Steeves and L.R. Harris (Eds.), *Plasticity in sensory systems* (pp. 94-108). Cambridge, UK: Cambridge University Press.

Kelly, K. R., Zohar, S. R., Gallie, B. L., & Steeves, J. K. E. (2013). Impaired speed perception but intact luminance contrast perception in people with one eye. *Investigative Ophthalmology & Visual Science*, *54*(4), 3058-3064.

Kier, E. L., Staib, L. H., Davis, L. M., & Bronen, R. A. (2004). MR imaging of the temporal stem: anatomic dissection tractography of the uncinate fasciculus, inferior occipitofrontal fasciculus, and Meyer's loop of the optic radiation. *American Journal of Neuroradiology*, *25*(5), 677-691.

Kikinis, Z., Makris, N., Finn, C. T., Bouix, S., Lucia, D., Coleman, M. J., ... & Kubicki, M. (2013). Genetic contributions to changes of fiber tracts of ventral visual stream in 22q11. 2 deletion syndrome. *Brain Imaging and Behavior*, *7*(3), 316-325.

Kim, D. J., Park, S. Y., Kim, J., Lee, D. H., & Park, H. J. (2009). Alterations of white matter diffusion anisotropy in early deafness. *Neuroreport*, *20*(11), 1032-1036.

Kinney, H. C., Kloman, A. S., & Gilles, F. H. (1988). Sequence of central nervous system myelination in human infancy. II. Patterns of myelination in autopsied infants. *Journal of Neuropathology & Experimental Neurology*, *47*(3), 217-234.

Kinoshita, Y., Ohnishi, A., Kohshi, K., & Yokota, A. (1999). Apparent diffusion coefficient on rat brain and nerves intoxicated with methylmercury. *Environmental Research*, *80*(4), 348-354.

Koldewyn, K., Yendiki, A., Weigelt, S., Gweon, H., Julian, J., Richardson, H., ... & Kanwisher, N. (2014). Differences in the right inferior longitudinal fasciculus but no general disruption of white matter tracts in children with autism spectrum disorder. *Proceedings of the National Academy of Sciences*, *111*(5), 1981-1986.

Le Bihan, D. (2003). Looking into the functional architecture of the brain with diffusion MRI.

Nature Reviews Neuroscience, *4*(6), 469-480.

Lebel, C. & Beaulieu, C. (2011). Longitudinal development of human brain wiring continues from childhood into adulthood. *The Journal of Neuroscience*, *31*(30), 10937-10947.

Lebel, C., Caverhill-Godkewitsch, S., & Beaulieu, C. (2010). Age-related regional variations of the corpus callosum identified by diffusion tensor tractography. *Neuroimage*, *52*(1), 20-31.

Lepage, M., Habib, R., & Tulving, E. (1998). Hippocampal PET activations of memory encoding and retrieval: the HIPER model. *Hippocampus*, *8*(4), 313-322.

Leporé, N., Shi, Y., Leporé, F., Fortin, M., Voss, P., Chou, Y. Y., ... & Thompson, P. M. (2009). Pattern of hippocampal shape and volume differences in blind subjects. *Neuroimage*, *46*(4), 949-957.

Leporé, N., Voss, P., Leporé, F., Chou, Y. Y., Fortin, M., Gougoux, F., ... & Toga, A. W. (2010). Brain structure changes visualized in early-and late-onset blind subjects. *Neuroimage*, *49*(1), 134-140.

Lessard, N., Pare, M., Leporé, F., & Lassonde, M. (1998). Early blind human subjects localize sound sources better than sighted subjects. *Nature, 395*(6699)*,* 278-80.

Li, J., Liu, Y., Qin, W., Jiang, J., Qiu, Z., Xu, J., ... & Jiang, T. (2013). Age of onset of blindness affects brain anatomical networks constructed using diffusion tensor tractography. *Cerebral Cortex*, *23*(3), 542-551.

Li, Q., Zhai, L., Jiang, Q., Qin, W., Li, Q., Yin, X., & Guo, M. (2015). Tract-based spatial statistics analysis of white matter changes in children with anisometropic amblyopia. *Neuroscience Letters*, *597*, 7-12.

Liu, Y., Yu, C., Liang, M., Li, J., Tian, L., Zhou, Y., ... & Jiang, T. (2007). Whole brain

functional connectivity in the early blind. *Brain*, *130*(8), 2085-2096.

Lund, R. D., Cunningham, T. J., & Lund, J. S. (1973). Modified optic projections after unilateral eye removal in young rats. *Brain, Behavior and Evolution*, *8*(1-2), 51-72.

Lutz, J., Hemminger, F., Stahl, R., Dietrich, O., Hempel, M., Reiser, M., & Jäger, L. (2007). Evidence of subcortical and cortical aging of the acoustic pathway: a diffusion tensor imaging (DTI) study. *Academic Radiology*, *14*(6), 692-700.

Maguire, E. A., Gadian, D. G., Johnsrude, I. S., Good, C. D., Ashburner, J., Frackowiak, R. S., & Frith, C. D. (2000). Navigation-related structural change in the hippocampi of taxi drivers. *Proceedings of the National Academy of Sciences*, *97*(8), 4398-4403.

Makris, N., Goldstein, J. M., Kennedy, D., Hodge, S. M., Caviness, V. S., Faraone, S. V., ... & Seidman, L. J. (2006). Decreased volume of left and total anterior insular lobule in schizophrenia. *Schizophrenia Research*, *83*(2), 155-171.

Makris, N., Kennedy, D. N., McInerney, S., Sorensen, A. G., Wang, R., Caviness, V. S., & Pandya, D. N. (2005). Segmentation of subcomponents within the superior longitudinal fascicle in humans: a quantitative, in vivo, DT-MRI study. *Cerebral Cortex*, *15*(6), 854-869.

Mandelstam, S. A. (2012). Challenges of the anatomy and diffusion tensor tractography of the Meyer loop. *American Journal of Neuroradiology*, *33*(7), 1204-1210.

Manford, M. & Andermann, F. (1998). Complex visual hallucinations. Clinical and neurobiological insights. *Brain*, *121*(10), 1819-1840.

Martino, J., Brogna, C., Robles, S. G., Vergani, F., & Duffau, H. (2010). Anatomic dissection of the inferior fronto-occipital fasciculus revisited in the lights of brain stimulation data. *Cortex*, *46*(5), 691-699.

Merabet, L. B. & Pascual-Leone, A. (2010). Neural reorganization following sensory loss: the opportunity of change. *Nature Reviews Neuroscience*, *11*(1), 44-52.

Michelson, G., Engelhorn, T., Wärntges, S., El Rafei, A., Hornegger, J., & Doerfler, A. (2013). DTI parameters of axonal integrity and demyelination of the optic radiation correlate with glaucoma indices. *Graefe's Archive for Clinical and Experimental Ophthalmology*, *251*(1), 243-253.

Mori, S. (2007). *Introduction to diffusion tensor imaging*. Amsterdam, NL: Elsevier.

Mori, S. & van Zijl, P. (2002). Fiber tracking: principles and strategies-a technical review. *NMR in Biomedicine*, *15*(7-8), 468-480.

Mori, S., Wakana, S., Van Zijl, P. C., & Nagae-Poetscher, L. M. (2005). *MRI atlas of human white matter*. Amsterdam, NL: Elsevier.

Mori, S. & Zhang, J. (2006). Principles of diffusion tensor imaging and its applications to basic neuroscience research. *Neuron*, *51*(5), 527-539.

Moro, S. S., Kelly, K. R., McKetton, L., Gallie, B. L., & Steeves, J. K. E. (2015). Evidence of multisensory plasticity: asymmetrical medial geniculate body in people with one eye. *Neuroimage: Clinical*, *9*, 513-518.

Moro, S. S. & Steeves, J. K. E. (2012). No Colavita effect: Equal auditory and visual processing in people with one eye. *Experimental Brain Research, 216*(3), 367-373.

Moro, S. S. & Steeves, J. K. E (2013). No Colavita effect: Increasing temporal load maintains equal auditory and visual processing in people with one eye. *Neuroscience Letters, 556*, 186-90.

Moro, S. S., Steeves, J. K. E., & Harris, L. R. (2014). Optimal audiovisual processing in people with one eye. *Multisensory Research*, *27*(3-4), 173-188.

Murai, H., Suzuki, Y., Kiyosawa, M., Tokumaru, A. M., Ishii, K., & Mochizuki, M. (2013). Positive correlation between the degree of visual field defect and optic radiation damage in glaucoma patients. *Japanese Journal of Ophthalmology*, *57*(3), 257-262.

Nicholas, J., Heywood, C. A., & Cowey, A. (1996). Contrast sensitivity in one-eyed subjects. *Visual Research, 26*(1), 175-180.

Nys, J., Scheyltjens, I., & Arckens, L. (2015). Visual system plasticity in mammals: the story of monocular enucleation-induced vision loss. *Frontiers in Systems Neuroscience*, *9*(60), 0-60.

O'Brien, B. J. & Olavarria, J. F. (1994). Anomalous patterns of callosal connections develop in visual cortex of monocularly enucleated hamsters. *Biological Research*, *28*(3), 211-218.

O'Donnell, L. J. & Westin, C. F. (2011). An introduction to diffusion tensor image analysis. *Neurosurgery Clinics of North America*, *22*(2), 185-196.

Olavarria, J. & Malach, R. (1987). Development of visual callosal connections in neonatally enucleated rats. *Journal of Comparative Neurology*, *260*(3), 321-348.

Park, H. J., Westin, C. F., Kubicki, M., Maier, S. E., Niznikiewicz, M., Baer, A., ... & Shenton, M. E. (2004). White matter hemisphere asymmetries in healthy subjects and in schizophrenia: a diffusion tensor MRI study. *Neuroimage*, *23*(1), 213-223.

Pierpaoli, C. & Basser, P. J. (1996). Toward a quantitative assessment of diffusion anisotropy. *Magnetic Resonance in Medicine*, *36*(6), 893-906.

Pinel, J. P. J. (2011). *Biopsychology* (8th ed.). Boston, MA: Allyn & Bacon.

Poggio, T., Fahle, M., & Edelman, S. (1992). Fast perceptual learning in visual hyperacuity. *Science, 256*(5059)*,* 1018-1021.

Putnam, M. C., Steven, M. S., Doron, K. W., Riggall, A. C., & Gazzaniga, M. S. (2010). Cortical

projection topography of the human splenium: hemispheric asymmetry and individual differences. *Journal of Cognitive Neuroscience*, *22*(8), 1662-1669.

Rakic, P. (1981). Development of visual centers in the primate brain depends on binocular competition before birth. *Science*, *214*(4523), 928-931.

Rakic, P. (1988). Specification of cerebral cortical areas. *Science*, *241*(4862), 170-176.

Reed, M. J., Steeves, J. K. E., Kraft, S. P., Gallie, B. L., & Steinbach, M. J. (1996). Contrast letter thresholds in the non-affected eye of strabismic and unilateral eye enucleated children. *Vision Research, 36*(18), 3011-3018.

Reed, M. J., Steeves, J. K. E., & Steinbach, M. J. (1997). A comparison of contrast letter thresholds in unilateral eye enucleated subjects and binocular and monocular control subjects. *Vision Research, 37*(17), 2465-2469.

Reed, M. J., Steinbach, M. J., Anstis, S. M., Gallie, B. L., Smith, D. R., & Kraft, S. P. (1991). The development of optokinetic nystagmus in strabismic and monocularly enucleated subjects. *Behavioural Brain Research, 46*(1), 31-42.

Reed, M. J., Steinbach, M. J., Ono, H., Kraft, S. & Gallie, B. (1995). Alignment ability of strabismic and eye enucleated subjects on the horizontal and oblique meridians. *Vision Research, 35*(17), 2523-2528.

Revill, K. P., Namy, L. L., DeFife, L. C., & Nygaard, L. C. (2014). Cross-linguistic sound symbolism and crossmodal correspondence: evidence from fMRI and DTI. *Brain and Language*, *128*(1), 18-24.

Roberts, T. P., Khan, S. Y., Blaskey, L., Dell, J., Levy, S. E., Zarnow, D. M., & Edgar, J. C. (2009). Developmental correlation of diffusion anisotropy with auditory-evoked response. *Neuroreport*, *20*(18), 1586-1591.

Ross, B. & Bluml, S. (2001). Magnetic resonance spectroscopy of the human brain. *The Anatomical Record*, *265*(2), 54-84.

Saron, C. D., Foxe, J. J., & Simpson, G. V., & Vaughan, H. G. (2003). Interhemispheric visuomotor activation: spatiotemporal electrophysiology related to reaction time. In E. Zaidel & M. Iacoboni (Eds.), *The parallel brain: the cognitive neuroscience of the corpus callosum* (171-219). Cambridge, MA: MIT Press

Schmahmann, J. D. & Pandya, D. N. (2007). The complex history of the fronto-occipital fasciculus. *Journal of the History of the Neurosciences*, *16*(4), 362-377.

Schmierer, K., Wheeler-Kingshott, C. A., Boulby, P. A., Scaravilli, F., Altmann, D. R., Barker, G. J., ... & Miller, D. H. (2007). Diffusion tensor imaging of post mortem multiple sclerosis brain. *Neuroimage*, *35*(2), 467-477.

Schmithorst, V. J., Wilke, M., Dardzinski, B. J., & Holland, S. K. (2002). Correlation of white matter diffusivity and anisotropy with age during childhood and adolescence: a cross-sectional diffusion-tensor MR imaging study. *Radiology*, *222*(1), 212-218.

Schmithorst, V. J. & Yuan, W. (2010). White matter development during adolescence as shown by diffusion MRI. *Brain and Cognition*, *72*(1), 16-25.

Schulte, T., Sullivan, E. V., Müller-Oehring, E. M., Adalsteinsson, E., & Pfefferbaum, A. (2005). Corpus callosal microstructural integrity influences interhemispheric processing: a diffusion tensor imaging study. *Cerebral Cortex*, *15*(9), 1384-1392.

Sener, R. N. (2001). Diffusion MRI: apparent diffusion coefficient (ADC) values in the normal brain and a classification of brain disorders based on ADC values. *Computerized Medical Imaging and Graphics*, *25*(4), 299-326.

Sengpiel, F. & Kind, P. C. (2002). The role of activity in development of the visual system.

Current Biology, *12*(23), R818-R826.

Shimony, J. S., Burton, H., Epstein, A. A., McLaren, D. G., Sun, S. W., & Snyder, A. Z. (2006). Diffusion tensor imaging reveals white matter reorganization in early blind humans. *Cerebral Cortex*, *16*(11), 1653-1661.

Shook, B. L. & Chalupa, L. M. (1986). Organization of geniculocortical connections following prenatal interruption of binocular interactions. *Developmental Brain Research*, *28*(1), 47-62.

Shu, N., Li, J., Li, K., Yu, C., & Jiang, T. (2009a). Abnormal diffusion of cerebral white matter in early blindness. *Human Brain Mapping*, *30*(1), 220-227.

Shu, N., Liu, Y., Li, J., Li, Y., Yu, C., & Jiang, T. (2009b). Altered anatomical network in early blindness revealed by diffusion tensor tractography. *PloS One*, *4*(9), e7228.

Sinnett, S., Soto-Faraco, S., & Spence, C. (2008). The co-occurrence of multisensory competition and facilitation. *Acta Psychologica, 128*(1), 153-61.

Sloper, J. J. (1993). Competition and cooperation in visual development. *Eye*, *7*(3), 319-331.

Smith, S. M. (2002). Fast robust automated brain extraction. *Human Brain Mapping*, *17*(3), 143-155.

Smith, S. M., Jenkinson, M., Johansen-Berg, H., Rueckert, D., Nichols, T. E., Mackay, C. E., ... & Behrens, T. E. (2006). Tract-based spatial statistics: voxelwise analysis of multi-subject diffusion data. *Neuroimage*, *31*(4), 1487-1505.

Smith, S. M., Jenkinson, M., Woolrich, M. W., Beckmann, C. F., Behrens, T. E., Johansen-Berg, H., ... & Niazy, R. K. (2004). Advances in functional and structural MR image analysis and implementation as FSL. *Neuroimage*, *23*, S208-S219.

Song, S. K., Sun, S. W., Ju, W. K., Lin, S. J., Cross, A. H., & Neufeld, A. H. (2003). Diffusion

tensor imaging detects and differentiates axon and myelin degeneration in mouse optic nerve after retinal ischemia. *Neuroimage*, *20*(3), 1714-1722.

Song, S. K., Sun, S. W., Ramsbottom, M. J., Chang, C., Russell, J., & Cross, A. H. (2002). Dysmyelination revealed through MRI as increased radial (but unchanged axial) diffusion of water. *Neuroimage*, *17*(3), 1429-1436.

Song, S. K., Yoshino, J., Le, T. Q., Lin, S. J., Sun, S. W., Cross, A. H., & Armstrong, R. C. (2005). Demyelination increases radial diffusivity in corpus callosum of mouse brain. *Neuroimage*, *26*(1), 132-140.

Spence, C. (2009). Explaining the Colavita visual dominance effect. *Progress in Brain Research*, *176*, 245-258.

Spence, C., Parise, C., & Chen, Y. C. (2011). The Colavita visual dominance effect. In Murray, M. M. and Wallace, M. (eds.), *Frontiers in the neural bases of multisensory processes* (pp. 523-550). Boca Raton, FL: CRC Press.

Staempfli, P., Rienmueller, A., Reischauer, C., Valavanis, A., Boesiger, P., & Kollias, S. (2007). Reconstruction of the human visual system based on DTI fiber tracking. *Journal of Magnetic Resonance Imaging*, *26*(4), 886-893.

Steeves, J. K. E., Gray, R., Steinbach, M. J., & Regan, D. (2000). Accuracy of estimating time to collision using only monocular information in unilaterally enucleated observers and monocularly viewing normal controls. *Vision Research*, *40*(27), 3783-3789.

Steeves, J. K. E., González, E. G., Gallie, B. L., & Steinbach, M. J. (2002). Early unilateral enucleation disrupts motion processing. *Vision Research, 42*(1), 143-150.

Steeves, J. K. E., González, E. G., & Steinbach, M. J. (2008). Vision with one eye: a review of visual function following monocular enucleation. *Spatial Vision, 21*(6)*,* 509-529.

Steeves, J. K. E., Wilkinson, F., González, E. G., Wilson, H. R., & Steinbach, M. J. (2004). Global shape discrimination at reduced contrast in enucleated observers. *Vision Research, 44*(9), 943-949.

Takahashi, M., Ono, J., Harada, K., Maeda, M., & Hackney, D. B. (2000). Diffusional anisotropy in cranial nerves with maturation: quantitative evaluation with diffusion MR imaging in rats. *Radiology*, *216*(3), 881-885.

Takao, H., Abe, O., Yamasue, H., Aoki, S., Sasaki, H., Kasai, K., ... & Ohtomo, K. (2011). Gray and white matter asymmetries in healthy individuals aged 21-29 years: a voxel-based morphometry and diffusion tensor imaging study. *Human Brain Mapping*, *32*(10), 1762-1773.

Tavor, I., Yablonski, M., Mezer, A., Rom, S., Assaf, Y., & Yovel, G. (2014). Separate parts of occipito-temporal white matter fibers are associated with recognition of faces and places. *Neuroimage*, *86*, 123-130.

Toldi, J., Fehér, O., & Wolff, J. R. (1996). Neuronal plasticity induced by neonatal monocular (and binocular) enucleation. *Progress in Neurobiology*, *48*(3), 191-218.

Toosy, A. T., Werring, D. J., Plant, G. T., Bullmore, E. T., Miller, D. H., & Thompson, A. J. (2001). Asymmetrical activation of human visual cortex demonstrated by functional MRI with monocular stimulation. *Neuroimage*, *14*(3), 632-641.

Tournier, J. D., Mori, S., & Leemans, A. (2011). Diffusion tensor imaging and beyond. *Magnetic Resonance in Medicine*, *65*(6), 1532-1556.

Trevelyan, A. J. & Thompson, I. D. (1992). Altered topography in the geniculo-cortical projection of the golden hamster following neonatal monocular enucleation. *European Journal of Neuroscience*, *4*(11), 1104-1111.

Tuch, D. S., Salat, D. H., Wisco, J. J., Zaleta, A. K., Hevelone, N. D., & Rosas, H. D. (2005). Choice reaction time performance correlates with diffusion anisotropy in white matter pathways supporting visuospatial attention. *Proceedings of the National Academy of Sciences of the United States of America*, *102*(34), 12212-12217.

Van Essen, D. C. (1997). A tension-based theory of morphogenesis and compact wiring in the central nervous system. *Nature*, *385*(6614), 313-318.

Verhoeven, J. S., Sage, C. A., Leemans, A., Van Hecke, W., Callaert, D., Peeters, R., ... & Sunaert, S. (2010). Construction of a stereotaxic DTI atlas with full diffusion tensor information for studying white matter maturation from childhood to adolescence using tractography-based segmentations. *Human Brain Mapping*, *31*(3), 470-486.

Wakana, S., Caprihan, A., Panzenboeck, M. M., Fallon, J. H., Perry, M., Gollub, R. L., … & Blitz, A. (2007). Reproducibility of quantitative tractography methods applied to cerebral white matter. *Neuroimage*, *36*(3), 630-644.

Welch, R. B. & Warren, D. H. (1980). Immediate perceptual response to intersensory discrepancy. *Psychological Bulletin, 88*(3)*,* 638-667.

Westlye, L. T., Walhovd, K. B., Dale, A. M., Bjørnerud, A., Due-Tønnessen, P., Engvig, A., ... & Fjell, A. M. (2009). Life-span changes of the human brain white matter: diffusion tensor imaging (DTI) and volumetry. *Cerebral Cortex*, *20*(9), 2055-2068.

Wittenberg, G. F., Werhahn, K. J., Wassermann, E. M., Herscovitch, P., & Cohen, L. G. (2004). Functional connectivity between somatosensory and visual cortex in early blind humans. *European Journal of Neuroscience*, *20*(7), 1923-1927.

Woolrich, M. W., Jbabdi, S., Patenaude, B., Chappell, M., Makni, S., Behrens, T., ... & Smith, S. M. (2009). Bayesian analysis of neuroimaging data in FSL. *Neuroimage*, *45*(1), S173-

S186.

Wu, Y., Sun, D., Wang, Y., & Wang, Y. (2016). Subcomponents and connectivity of the inferior fronto-occipital fasciculus revealed by diffusion spectrum imaging fiber tracking. *Frontiers in Neuroanatomy*, *10*(88), 1-13.

Xie, S., Gong, G. L., Xiao, J. X., Ye, J. T., Liu, H. H., Gan, X. L., ... & Jiang, X. X. (2007). Underdevelopment of optic radiation in children with amblyopia: a tractography study. *American Journal of Ophthalmology*, *143*(4), 642-646.

Yakovlev, P. I. & Lecours, A. R. (1967). The myelogenetic cycles of regional maturation of the brain. In: Minkowski A. (Ed.). *Regional development of the brain in early life* (3-79). Oxford, UK: Blackwell Scientific.

Yogarajah, M., Focke, N. K., Bonelli, S., Cercignani, M., Acheson, J., Parker, G. J. M., ... & Duncan, J. S. (2009). Defining Meyer's loop – temporal lobe resections, visual field deficits and diffusion tensor tractography. *Brain*, *132*(6), 1656-1668.

Yu, C., Liu, Y., Li, J., Zhou, Y., Wang, K., Tian, L., ... & Li, K. (2008). Altered functional connectivity of primary visual cortex in early blindness. *Human Brain Mapping*, *29*(5), 533-543.

Yu, C., Shu, N., Li, J., Qin, W., Jiang, T., & Li, K. (2007). Plasticity of the corticospinal tract in early blindness revealed by quantitative analysis of fractional anisotropy based on diffusion tensor tractography. *Neuroimage*, *36*(2), 411-417.

Zhang, Y., Suga, N., & Yan, J. (1997). Corticofugal modulation of frequency processing in bat auditory system. *Nature*, *387*(6636), 900-903.

Zhang, Q. J., Wang, D., Bai, Z. L., Ren, B. C., & Li, X. H. (2015). Diffusion tensor imaging of optic nerve and optic radiation in primary chronic angle-closure glaucoma using 3T

magnetic resonance imaging. *International Journal of Ophthalmology*, *8*(5), 975.

Zikou, A. K., Kitsos, G., Tzarouchi, L. C., Astrakas, L., Alexiou, G. A., & Argyropoulou, M. I. (2012). Voxel-based morphometry and diffusion tensor imaging of the optic pathway in primary open-angle glaucoma: a preliminary study. *American Journal of Neuroradiology*, *33*(1), 128-134.